



Phytochemical-Based Evidence of the Health Benefits of *Bidens Pilosa* Extracts and Cytotoxicity

Oladayo Amed Idris^{1,5} · Nasifu Kerebba^{2,3} · Suranie Horn^{1,4} · Mark Steve Maboeta¹ · Rialet Pieters¹

Received: 23 December 2022 / Accepted: 13 February 2023
© The Author(s) 2023

Abstract

Purpose *Bidens pilosa* L. is traditionally used as a flavouring agent in foods, in the treatment of diseases, in agriculture as a biopesticide and herbicide, and in the phytoremediation of soils contaminated with heavy metals. The vast range of uses of *B. pilosa* for a variety of purposes is questionable, hence motivating the objectives of this study, which are to assess the cytotoxicity, health benefits, and/or risks of *B. pilosa* using chemical-based evidence.

Methods A real-time cell analysis (xCELLigence system), ultra-high-performance liquid chromatography coupled to a quadrupole-time-of-flight mass spectrometer, high-performance liquid chromatography with a diode array detector, and chemical-based spectrophotometric methods were adopted in the study.

Results High concentrations of the ethanol extracts exhibited cytotoxic activity on HepG2 (cancerous), and Vero (non-cancerous) cell lines, whereas the water extracts promoted cell proliferation at selected concentrations. The chemical profiling enabled the separation as well as characterisation of 137 phytochemicals. These were mainly phenolic acids, flavonoids, fatty acids, coumarins, and furanocoumarins. There was no toxic compound identified.

Conclusion The ethanol extracts are generally more potent and exhibit stronger antioxidant activity and cytotoxicity, probably due to the presence of more flavonoids and phenolic acids, validating the uses of *B. pilosa* and its relevance as a source of functional phytochemicals.

Keywords Antioxidant · Cytotoxicity · Metabolite · Phytochemicals · Plant extracts · xCELLigence

1 Introduction

Bidens pilosa is an annual weed that is widely distributed in tropical and subtropical areas around the world due to its high tolerance to adverse environmental conditions [1]. It belongs to the Asteraceae family, has yellow flowers, and grows to a height of 30–100 cm. *B. pilosa* is used for

a variety of purposes around the world, including food and traditional medicine [2], plant biopesticide [3], phytoremediation of heavy metal-polluted soils [4, 5] and weed control [6].

Bidens pilosa has a rich ethnobotanical history. It has been reported to be traditionally used in sauce recipes and as an ingredient in tea [7]. It is used to treat hyperglycemia

✉ Mark Steve Maboeta
mark.maboeta@nwu.ac.za

Oladayo Amed Idris
dayoamed@yahoo.com

Nasifu Kerebba
nkerebba@gmail.com

Suranie Horn
suranie.horn@nwu.ac.za

Rialet Pieters
rialet.pieters@nwu.ac.za

¹ Unit for Environmental Sciences and Management (UESM), Faculty of Natural and Agricultural Sciences, North-West University, Private Bag X6001, Potchefstroom, North-West 2520, South Africa

² Department of Chemistry, Makerere University, P.O. Box 7062, Kampala, Uganda

³ Department of Chemistry, Kyambogo University, P.O. Box 1, Kyambogo, Uganda

⁴ Occupational Health and Hygiene Research Initiative, North-West University, Potchefstroom Campus 2520, South Africa

⁵ Division of Botany, Department of Animal and Plant Systematics, National Museum, Bloemfontein, South Africa

[8], malaria [9], tumours [10], microbial infections [11], rheumatoid arthritis, and inflammation [12]. Heavy metals such as arsenic and cadmium have been reported to bioaccumulate in *B. pilosa*, which suggests that the plant has the potential for the phytoremediation of heavy metals [4]. In the study of Salazar et al. (2021) [13], *B. pilosa* was reported to be effective in the removal of lead from contaminated soils [13]. The plant has also been used to control weeds through its allelopathic properties and to inhibit plant pathogens [6]. It has been reported that *B. pilosa* extracts improve crop yield by controlling insect pests on legume crops and significantly reducing stored grain pests [14, 15]. The essential oil produced by *B. pilosa* has been found to possess antimicrobial activities and free radical scavenging potential [16].

According to reports, *B. pilosa* is an effective insecticide, nematicide, and herbicide. This was confirmed by Ahmed et al. (2021) [14] that the methanolic extract of the plant has significant insecticidal activity against the grain beetle (*Oryzaephilus surinamensis* L.), bean weevil (*Acanthoscelides obtectus*) and rice weevil (*Sitophilus oryzae* L.) [14]. The no-choice test conducted by Mersie et al. (2019) [17] on Asteraceae weeds revealed that Parthenium beetle (also Mexican beetle) (*Zygogramma bicolorata*) avoids laying eggs on *B. pilosa* as much as they could and also does not feed on it [17]. In a two-day multiple-choice test carried out by Bajracharya et al. (2020) [18], *Z. bicolorata* avoided a few Asteraceae weeds including *B. pilosa* except *Parthenium hysterophorus* L. The extracts of *B. pilosa* significantly reduced the numbers of the Japanese pine sawyer (*Monochamus alternatus*) as well as the pine-wood nematode (*Bursaphelenchus xylophilus*) [19]. Due to the allelopathic characteristics of *B. pilosa* [6], the water extracts of the plant integrated with water irrigation have been found to effectively suppress weeds in a direct-seeded rice production system, which increases rice yield [20].

In ethnoveterinary medicine, *B. pilosa* has been reported to be effective in the treatment of several ailments in livestock. For instance, in Trinidad and British Columbia, Canada, *B. pilosa* is used to improve nutrition in horses [21]. According to Chang et al. (2016) [22], *B. pilosa* benefits chickens by improving growth through the modulation of gut bacteria, decreasing protozoan infection, and reducing caecal damage. The severity of liver fibrosis and injury in rats was reported to be reduced by *B. pilosa* when administered for 6 weeks [23], suggesting that it could be used to treat liver diseases. Fructose-induced hypertension and hypertriglyceridemia in rats were reversed by aqueous and methylene chloride extracts of *B. pilosa*, indicating that the plant extracts had hypotensive effects unrelated to insulin level modulation [24].

The bioactivities of *B. pilosa* are associated with its diverse phytochemicals, some of which have been identified as porphyrins, tannins, aliphatics, terpenoids, alkaloids, phenylpropanoids, cardiac glycosides, flavonoids, and aromatics [7]. There is a wide range of bioactive compounds present in the genus *Bidens*, however, the specific phenolic compounds present have not been fully elucidated. Generally, phytochemicals or plant secondary metabolites are used in the manufacture of food additives, pharmaceutical products, cosmetics, flavours, colognes, biopesticides and a variety of other products. However, most medicinal plants, including *B. pilosa*, are still not commercially grown, making it difficult to obtain plants which are the major natural source of secondary metabolites [25]. Although secondary metabolites are also produced by bacteria, fungi, and several marine organisms such as corals, sponges, and tunicates [26], plants still remain the most reliable source.

Given the vast range of uses of *B. pilosa* around the world, including food, traditional medicine, biopesticides, and herbicides, the health risks associated with the consumption of the plant are questionable. This leads to the aims of this study: to determine the cytotoxicity of *B. pilosa* and to use chemical-based evidence to determine the health benefits and/or risks as well as correlate the identified metabolites with the biological activities. To answer these questions, the phytochemicals in *B. pilosa* extracts were comprehensively characterized using ultra-high-performance liquid chromatography coupled to a quadrupole-time-of-flight mass spectrometer (UHPLC-ESI-Q-TOF-MS). The antioxidant content and activities were evaluated using spectrophotometric methods. Cytotoxicity of the extract was assessed on cancerous and non-cancerous cell lines utilizing a real-time cell analysis system (xCELLigence).

2 Materials and Methods

2.1 Plant Materials

The aerial parts of *B. pilosa* were collected from their natural habitat in Lepelle-Nkumpi Local Municipality, Limpopo (24° 19' 17" S, 29° 11' 1" E) Province, South Africa. Permission to collect the plant sample was granted by the landowner and Limpopo province. The samples of *Bidens pilosa* were identified by Professor Stefan Siebert, a Professor of Geobotany and the curator of the AP Goossens Herbarium, Faculty of Natural and Agricultural Sciences, North-West University. The voucher specimen of *B. pilosa* was deposited at the A.P. Goossens Herbarium and assigned the accession number 15,452 and barcode PUC0015452, then stored in the BRAHMS database. The authors abide by the International Union for Conservation of Nature (IUCN) policy, as

well as national and international guidelines and legislation, in the collection. The plant material was air-dried at room temperature before being pulverized. The moisture content of the pulverized samples was calculated using water mass to dry mass ratio of the pulverized samples. The initial mass (m) was determined before drying the samples, followed by the final mass (m_0) after drying the samples in an oven at 105°C until a constant mass was achieved. The water mass of the samples ($m - m_0$), and the moisture content (MC) were calculated using the formula:

$$MC = \frac{m - m_0}{m_0} \times 100\%$$

Extraction of phytochemicals was carried out by mixing the pulverized samples in ethanol-water solution (7:3, v/v) on a mechanical shaker for 48 h. The plant-to-solvent ratio was 1:10 (m/v). The extracts were filtered through Whatman® filter paper, Grade 1, (diameter 150 mm), concentrated with a rotary evaporator and dried by lyophilisation. The yield was calculated. Samples were then reconstituted in distilled water before being used but were suspended in 2 mL of 50% methanol (Sigma-Aldrich, ≥99.90% purity) and 0.1% formic acid (Sigma-Aldrich, reagent grade, ≥95%) prior to the MS analysis.

2.2 Antioxidant Content

2.2.1 Total Polyphenol Assessment

The total polyphenol content of the extracts was determined using the Folin-Ciocalteu reagent, with minor adjustments, as described by Daniels et al. (2015) [27]. The samples were prepared by serial dilution in the range of 10–100 mg/mL, while the standard curve was prepared in the range of 10–500 mg/mL gallic acid (Sigma-Aldrich, ≥98.5% purity) in 10% ethanol. An aliquot of 25 µL of the sample was pipetted into the wells of a transparent 96-well microplate, then mixed with 125 µL Folin-Ciocalteu reagent (1:10 v/v in distilled water). After 5 min., 100 µL of 7.5% m/v anhydrous sodium carbonate (Na_2CO_3) was added to the wells making the total volume to be 250 µL. The mixture was incubated for 2 h in the dark at room temperature after which absorbance was recorded at 765 nm using a Multiskan™ plate reader (Thermo Electron Corporation, USA). The assay was done in triplicate and the result was expressed as mg gallic acid-equivalents (GAE) per gram of extract's total polyphenol (mg GAE/g) based on the gallic acid standard curve [28].

2.2.2 Total Flavonol

The flavonol content was determined using the quercetin standard, as previously described [27], also using a spectrophotometric method. The standard linear calibration curve was obtained by preparing quercetin in 95% ethanol at concentrations ranging from 0, 5, 10, 20, 40, and 80 mg/L. In a 96-well microplate, 12.5 µL of the plant extracts was pipetted in a well, then mixed with 12.5 µL hydrochloric acid (0.1% HCl, v/v in 95% ethanol), and 225 µL hydrochloric acid (2% HCl, v/v in distilled water), making the total volume 250 µL. The mixture was then incubated for 30 min at room temperature. Absorbance was measured using a spectrophotometer (Multiskan™ plate reader, Thermo Electron Corporation, USA) in the dark at 25°C at 360 nm. This was done in triplicate for all of the samples. The total flavonol was expressed as mg quercetin-equivalents per g dry mass of extracts (mg QE/g) using the linearity of the quercetin standard.

2.3 Antioxidant Activities

2.3.1 2,2-Azino-di-3-ethylbenzthiazoline Sulfonate (ABTS) Assay

The 2,2-Azino-di-3-ethylbenzthiazoline sulfonate (ABTS) assay was used to quantify the radical scavenging activity of the samples adopting the method of Re et al. (1999) [29]. The stock solution was prepared by stoichiometrically reacting 7 mM ABTS with 2.45 mM potassium-persulfate ($\text{K}_2\text{S}_2\text{O}_8$) at a ratio of 1:0.5 in the dark at room temperature for 24 h to produce $\text{ABTS}^{+\cdot}$. Prior to the assay, the $\text{ABTS}^{+\cdot}$ solution was mixed with 96% ethanol at 30°C until an absorbance of 0.70 (± 0.02) was obtained at 734 nm [30]. Trolox (6-hydrox-2,5,7,8-tetramethylchroman-2-carboxylic acid) was used as the standard, and the standard curve was plotted in the concentration range (0–500 µM). Diluted $\text{ABTS}^{+\cdot}$ solution ($A_{734\text{nm}} = 0.700 \pm 0.02$) of 300 µL was added to 25 µL of the plant extracts and allowed to incubate in the dark at 30°C for 30 min before measuring absorbance at 734 nm. All tests were performed in triplicate at each concentration of the standard and samples. The results were expressed as µM trolox-equivalents per g dry mass (µM TE/g).

2.3.2 Ferric Reducing Antioxidant Power (FRAP) Assay

The ferric reducing antioxidant power (FRAP) assay was carried out using the method previously described by Daniels et al. (2015) [27]. FRAP reagent was prepared from a solution of 10 mL of 0.3 M acetate buffer (pH 3.6), 1 mL of 10 mM 2,4,6-tripyridyl-s-triazine (TPTZ) dissolved in 0.1 M HCl, and 1 mL of 20 mM iron (III) chloride

hexahydrate ($\text{FeCl}_3 \cdot 6\text{H}_2\text{O}$) dissolved in distilled water. In a 96-well microtiter plate, an aliquot of 10 μL of varying concentrations of plant extracts and standard (0–1000 μM) was pipetted and mixed with 300 μL FRAP reagent. The mixture was incubated at 37°C for 30 min and absorbance was read at 593 nm. L-Ascorbic Acid was used as the standard, and the results were expressed as μM ascorbic acid-equivalents per g dry mass (μM AAE/g).

2.4 Quantification of Phytochemicals and Profiling

The preliminary profiling of *B. pilosa* extracts was carried out using high-performance liquid chromatography with diode-array detection (HPLC-DAD), an Agilent 1200 Series HPLC device (Agilent, Santa Clara, USA), and a photodiode array detector. The phytochemicals of the plant extracts were identified and quantified using a Waters Synapt G2 qTOF mass spectrometer (Waters, Milford, MA, USA). Before injection, all samples were filtered through a 0.45 μm filter (Nylon Membranes, Supelco, Bellefonte, USA).

2.4.1 Method for HPLC-DAD Analysis

An HPLC-DAD with a reverse-phase RP-18 HS C18 discovery column (150 mm x 4.6 mm i.d., 5 μm , column temperature: room temperature) was used as previously described with minor modifications for preliminary profiling by Zeb (2015) [31]. The mobile phase consisted of water containing 0.1% trifluoroacetic acid (A), and methanol containing 0.1% trifluoroacetic acid (B), and then the flow rate was set at 1 mL/min. The elution program was performed with a gradient starting at 0 min, 100% of A, moving to 100% of B after 25 min. The detected wavelengths were recorded at three different UV channels; 280, 320, and 360 nm. The injection volume was 20 μL . The HPLC-DAD system was allowed to warm up before each run, and the baseline was monitored until it was stable before sample analysis. Peak identification was accomplished by comparing the retention duration and UV absorption spectra obtained with the standards.

2.4.2 Method for Liquid Chromatography-mass Spectrometry (LCMS) Analysis

A Waters Synapt G2 Quadrupole time-of-flight (QTOF) mass spectrometer (MS) connected to a Waters Acquity ultra-performance liquid chromatograph (UPLC) (Waters, Milford, MA, USA) was used for high-resolution UPLC-MS analysis. Electrospray ionization was carried out in both negative and positive modes with a cone voltage of 15 V, a desolvation temperature of 275 °C, a desolvation gas flow

rate of 650 L/h, and the rest of the MS settings optimised for best resolution and sensitivity. Data were acquired by scanning from m/z 150 to 1500 in resolution mode as well as in MSE mode. In MSE mode, two channels of MS data were acquired, one at low collision energy (4 V) and the second collision energy ramp at 40–100 V to obtain fragmentation data. Leucine enkephalin was used as a lock mass (reference mass) for accurate mass determination, and the instrument was calibrated with sodium formate. A volume of 2 μL was injected. The mobile phase consisted of water solvent A and acetonitrile (solvent B). Both solvent lines contained 0.1% formic acid. The gradient started at 100% solvent A for 1 min, reaching 28% B over 22 min in a linear way, then 40% B over 50 s and a wash step of 1.5 min at 100% B, followed by re-equilibration to initial conditions for 4 min. The flow rate was set to 0.25 mL/min, and the column temperature was held constant at 55 °C. Separation was achieved on a Waters BEH C18, 2.1 \times 100 mm, 1.7 μm column.

Based on the following three criteria, compounds were identified and assigned tentative names of identity. (1) Accurate mass match: the masses were automatically matched using XCMS, which was linked to Metlin (http://metlin.scripps.edu/metabo_search.php), MassBank, NIST, and other libraries. All compounds whose accurate mass error (AME) is > 5 ppm was considered unidentified [32]. (2) Mass fragmentation patterns: if available, the mass fragmentation patterns of the compounds are searched in the aforementioned databases. A few phenolic compound standards were spiked under similar LC-MS conditions and fragmentation patterns were compared to identify a given compound based on the retention time, mass fragmentation, and ionisation modes i.e. (by corresponding ions of protonated and deprotonated moieties). Since many compounds could be identified by UPLC-ESI-QTOF-MS, it was not possible to obtain all standards. Therefore, other similar compounds' MS and MS² fragment ions in literature and databases were used for the annotation of the compounds. (3) The number of carbon atoms in the peak: the carbon atoms were calculated if isotope abundances were available. The predicted number of carbon atoms in the putatively identified compound was used to reduce false annotations.

2.4.3 Analytical Protocols and Validation Procedure

The developed UHPLC-MS method was validated with a linearity curve, the limit of detection (LOD), the limit of quantification (LOQ), precision, and recovery according to the International Conference on Harmonization (ICH) recommendations [33]. Different concentrations of the standard mixture (3.906, 7.813, 15.63, 31.25, 62.5.0, 125.0, and 250.0 mg/L), which were approximated as 3.9, 7.8, 15.6, 31.3, 62.5, 125.0, and 250.0 mg/L, respectively, were

injected for quantification. The linearity of the calibration curve was checked by plotting the peak areas against the series of standard solution concentrations (mg/L) and determining the correlation coefficient using a linear regression model. In all cases, the system was linear ($r > 0.99$). LOD and LOQ were calculated by the parameters of the analytical curves (standard deviation of the response and slope). The standard deviation of the y-intercepts of regression lines was used as the standard deviation of the blank. The LODs and LOQs were estimated as 3.3 and 10 times the standard deviation of the blank/slope ratio of the calibration curve, respectively.

The repeatability of *B. pilosa* samples was assessed by using intraday and interday variations, and the relative standard deviation (RSD) was taken as a measure of precision. The intraday and interday variations were analysed using six replicates during a single day and by duplicating the experiments on three consecutive days. The percentage relative standard deviations (%RSD) of the peak areas (UV detection) and retention times were determined for each peak detected. The intraday repeatability (expressed as %RSDs) of the retention times was in the range of 0.14 to 3.14%, whereas the interday repeatability was from 1.01 to 2.90%. The intraday repeatability (expressed as %RSDs) of the total peak area was 0.32–0.70%, whereas the interday repeatability was 1.01–1.13%.

The recovery test was done by adding the known amounts of standards at low (50% of the known amounts), medium (same as the known amounts) and high (150% of the known amounts) levels into samples to evaluate the accuracy of the method. This was applied in triplicate.

2.5 Cytotoxicity Using Real-time Cell Analysis (RTCA)

2.5.1 Maintenance of Cells

Cell lines from the human liver, HepG2 (cancerous), and African monkey kidney, Vero (non-cancerous), were used to measure the cytotoxic potential of *B. pilosa* extracts (water and 70% ethanol). Since different cell lines originate from different organ tissues and these organs have different sensitivities towards compounds, the measured cytotoxic responses may be dependent on the cell type used [34]. The HepG2 liver cell line was chosen because one of the main functions of the liver is detoxification. These cells are immortalised and universally used as a model to assess toxic potency. Although the origin of the Vero, non-cancerous cells are different (kidney), both the liver and kidneys are involved in the excretion of substances from the body [35]. Both cell lines were obtained from the American Type Culture Collection (Manassas, VA, USA) (HB-8065 and CCL-81

respectively). The cells were grown in Dulbecco's Modified Eagle's Medium (DMEM) (Sigma, Darmstadt) supplemented with 10% fetal bovine serum (FBS) (Thermo Scientific, USA) in a humidified incubator with 5% CO₂ at 37 °C. Cells were handled in a sterile laminar flow hood, which was cleaned with 70% ethanol [36].

2.5.2 xCELLigence Cell Proliferation Assay

The impedance technology of the xCELLigence system (Real-Time Cell Analyser-RTCA; ACEA Biosciences Inc., San Diego, USA) with RTCA software (version 1.2.1) was used to monitor the cytotoxic effects of *B. pilosa* on two adherent cell lines (HepG2 and Vero) for 24 h. The system provides proliferation profiles as cells interact with the microelectrodes, allowing the IC₅₀/EC₅₀ values to be calculated. Cell growth is measured in real-time and converted into cell index (CI) values. Others have also documented using this method [37–39]. The HepG2 and Vero cells were seeded at a density of 5×10^4 cells/mL in the 96-well gold-plated E-plate and left to adhere for a period of 24 h. The cells were exposed to a concentration range of 15.6, 31.25, 62.5, 125, 250, 500, and 1000 µg/mL of reconstituted plant material after extraction with two solvents (See Sect. 2.1) in triplicate. The unexposed (control) cells received DMEM culture medium only.

2.6 Statistical Analyses

The significant differences in the data obtained in antioxidant content and activity were evaluated by two-way analysis of variance (ANOVA), ($p < 0.05$), using GraphPad Prism® 8.0.1. The results were presented as means \pm standard deviation. In the cytotoxicity, the cell index data obtained after the exposure was normalised with RTCA data analysis software. Normalisation was done at a specific time point (start of the test compound treatment), which was then set as 1.0 by the software and all the other values are represented as a proportion of this value. The dose-response curve and the EC₅₀ values were obtained using the xCELLigence system's RTCA-integrated software. The EC₅₀ value was calculated in the RTCA software under the analysis profile by selecting the exposure period. The data are presented as mean [$\mu\text{g/mL}$] \pm standard deviation ($n = 5$).

3 Results

3.1 Phytochemical Yields and Moisture Content

The extract yields from the plant correlated with the solvent type, with the ethanol-water (7:3, v/v) extracting

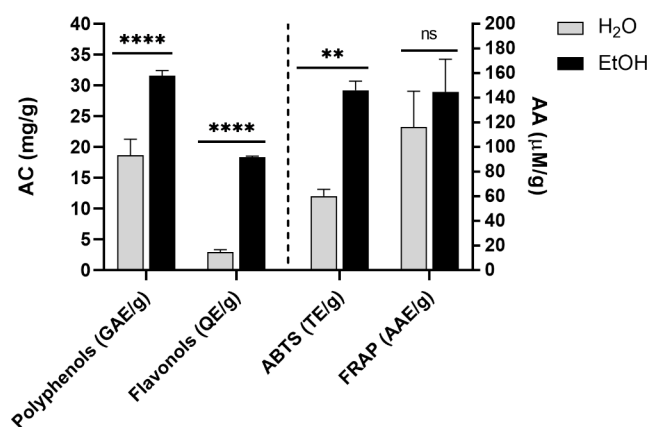


Fig. 1 The antioxidant content (AC) and antioxidant activity (AA) of *Bidens pilosa*. The values represent the mean \pm standard deviation of the phytochemicals (polyphenols and flavonols) and antioxidant activities (ABTS and FRAP) of the water (H₂O) and 70% ethanol (EtOH) extracts of *B. pilosa*. **** $p < 0.0001$; ** $p = 0.0035$, n.s = not significant, $p = 0.3675$. ABTS = 2,2-Azino-di-3-ethylbenzthiazoline sulfonate; FRAP = ferric reducing antioxidant power; GAE = gallic acid equivalents; QE = quercetin equivalents; TE = Trolox equivalents; AAE = ascorbic acid equivalents

significantly more than the water. The ethanol-water extract yield was $14.55 \pm 0.86\%$, whereas the water yield was $8.49 \pm 0.28\%$. The yields from both solvents are notably different, which could be attributable to the characteristics of these solvents. The residual moisture of the pulverized plant sample was determined after drying. The moisture content of the pulverised samples was evaluated to be 5.14% dry matter.

3.2 Antioxidant Content and Activity

The antioxidant content concentration (total polyphenol and total flavonol) varies depending on the extraction (water extract and 70% ethanol extract). Similarly, there was a strong relationship between the phytochemicals and antioxidant activity in the test samples. Figure 1 show that the concentration of the phytochemicals in the ethanol samples is higher compared to the water samples, and this has an obvious ripple effect on the antioxidant activities. It indicates that the ethanol extracts were more potent than the water extracts. The concentrations of the total polyphenols ranged from 15.66 to 20.19 mg GAE/g in the water extract and from 30.86 to 32.52 mg GAE/g for the ethanol extract, with mean values of 18.65 mg GAE/g and 31.56 mg GAE/g respectively. The mean value of the flavonol content of the water extract is 2.92 mg QE/g while the ethanol extract is 18.31 mg QE/g. The antioxidant activities of the ethanol extracts are higher, indicating a higher potency, and they correlate with the phytochemical concentrations. The antioxidant activities of water extracts of ABTS and FRAP are $60.02 \mu\text{mol AAE/g}$ and $116.29 \mu\text{mol TE/g}$, respectively,

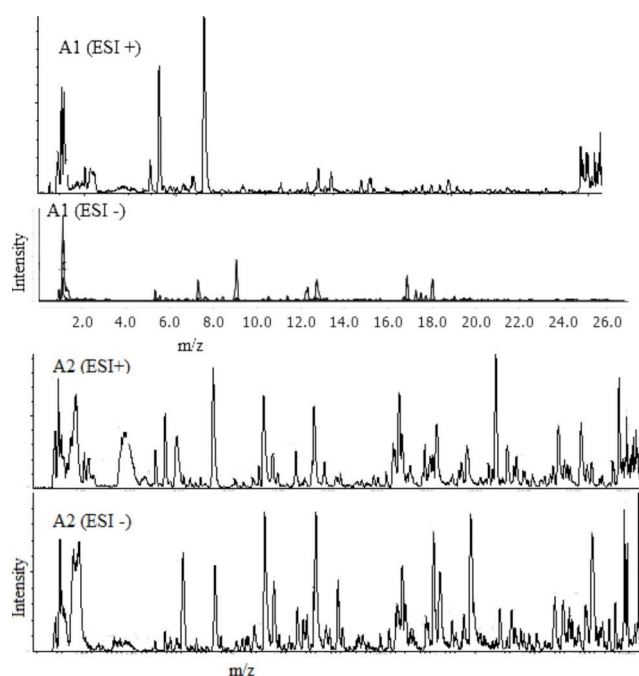


Fig. 2 UHPLC-ESI-MS base peak chromatogram for water (A1) and 70% ethanol (A2) of extracts of *Bidens pilosa* analysed in the negative and positive ion modes

while the ethanol activities are $146.02 \mu\text{mol AAE/g}$ and $144.81 \mu\text{mol TE/g}$.

3.3 Qualitative Analysis of Phytochemicals Using UHPLC-MS and HPLC-DAD

Due to the overlapping of numerous compounds, particularly in the phenolic fraction, HPLC-DAD produces complex profiles of the compound fraction. Nevertheless, UPLC-MS could exclude interferences using MS modes and product ion scan thus verifying the structure of the compound. The examination of base peak chromatograms of *B. pilosa* extracts shown in Fig. 2 enabled phytochemicals to be screened. In this study, UHPLC-ESI-MS enabled the detection of a total of 137 peaks (Table 1).

3.3.1 Characterisation of Phenolic Acids and Their Derivatives

3.3.1.1 Hydroxybenzoic Acids Twelve benzoic acid derivatives with peaks (19, 20, 21, 22, 24, 33, 43, 73, 80, 81, 101 and 120) were identified. Peak 19 was identified in the negative ion mode. It reveals a deprotonated molecular ion, $[\text{M-H}]^-$ at m/z 153 and upon collision inductive dissociation (CID), fragments m/z 123 $[\text{M-H}-2\text{CH}_3]^-$ and 109 $[\text{M-H}-\text{CO}_2]^-$ were formed, enabling tentative identification (dihydroxy benzoic acid) using the NIST database and literature [40]. Peak 22 has $[\text{M-H}]^-$ at m/z 167 and produced a

Table 1 Phytochemicals screened from water and 70% ethanol extracts of *Bidens pilosa*

Peak no	t _R (min)	Molecular formula	UV λ _{max} (nm)	(M-H) ⁻ /(M+H) ⁺ (m/z)	MS/MS product ions (m/z)	Tentative identification	Sample
1 ^b	0.90	C ₁₀ H ₈ O ₂	294	158.9788	115, 131, 116	Methylcoumarin	A2, A1
2 ^c	1.06	C ₁₂ H ₁₀ O ₄	267	219.0265*	192, 175	Hydro xanthotoxin	A2, A1
3 ^b	1.10	C ₇ H ₁₂ O ₆	267	191.0567	149, 165, <u>179</u> , 135	quinic acid	A2, A1
4	1.10	C ₁₄ H ₁₇ O ₅	267	266.1258*	219, 248	Dimethylhydroxy hydrogenated xanthotoxin	A2
5 ^b	1.20	C ₁₀ H ₅ O ₃	267	175.1094*	163	Coumarin derivative	A2, A1
6 ^b	1.70	C ₇ H ₁₂ O ₆	267	191.0580	173, 131	Citric acid	A2, A1
7 ^b	1.80	C ₁₄ H ₁₄ O ₅	266	262.1284*	175	Diacetyl methoxycoumarin	A2, A1
8 ^b	1.90	C ₇ H ₁₂ O ₆	261	191.0204	173, 131	Citric acid	A2
9 ^b	2.10	C ₂₄ H ₁₇ O ₁₀		465.2140*	294, 232, 188, 166	5-Methoxy-8-hydroxypsoralen dimer	A1
10 ^b	2.30	C ₁₅ H ₁₈ O ₈		325.1152*	289, 271, 163, 180, 145, 127	p-coumaric acid glucoside	A2
11 ^b	2.68	C ₁₄ H ₁₂ O ₄	261	243.0652	131, 142, 147, 186, 191, 200, 179	Piceatannol	A2
12 ^b	3.30	C ₇ H ₁₀ O ₆		173.0097	155, 149	Quinide	A2
13 ^b	4.60	C ₁₃ H ₁₄ O ₆	274	268.1042*	204	acetyl hydroxycoumarin derivative	A2
14 ^c	4.94	C ₄₂ H ₅₅ O ₂₇	272	989.3256	179, 383, 819, 665, 656, 760, 282, 161, 341, 145, 737, 899, 265	1-O-(2 ¹ -O-Coumaryl-1 ¹¹ -O-diglucosyl) caffeoyl-2 ¹¹¹ -O-diglucoside	A2
15 ^b	5.00	C ₁₅ H ₁₈ O ₈		325.1125*	289, 271, 163, 253, 223, 308	p-Coumaric acid glucoside	A2, A1
16 ^a	5.38	C ₉ H ₁₁ NO ₂	288	164.0709	153, 147, 109, 151	Phenylalanine	A2, A1
	5.38	C ₉ H ₁₁ NO ₂	288	166.0852*	120, 103	Phenylalanine	A2
17 ^b	5.60	C ₂₅ H ₂₃ O ₁₀		483.1286	301, 371, 277, 288, 339, 403, 173, 191	3,4-di-O-(E)-p-coumaroylquinic acid	A2, A1
18 ^b	5.80	C ₁₅ H ₁₈ O ₈	259	326.1266	236, 164, 173, 153, 278	p-Coumaric acid hexoside	A2
19 ^b	5.9	C ₇ H ₅ O ₄	261, 292	153.0196	123, 109	Dihydroxy benzoic acid	A1
20 ^b	6.10	C ₁₄ H ₂₀ O ₈	313	315.0715	<u>153</u> , 109	Dihydroxy benzoic acid -O-hexoside	A2, A1
21 ^b	6.40	C ₁₂ H ₁₁ O ₄	282	218.0913	<u>153</u>	Dihydroxy benzoic acid derivative	A1
22 ^b	6.59	C ₈ H ₈ O ₄	253, 288	167.0345	152, <u>123</u> , 108	Vanilic acid	A2
23 ^b	6.80	C ₁₇ H ₁₉ O ₁₀	274	382.0964	329, 311, 184, 149	Caftaric acid derivative	A1
	6.80	C ₁₇ H ₁₉ O ₁₀	274	384.1151*	252, 162, 192	Caftaric acid derivative	A1
24 ^b	7.30	C ₉ H ₁₀ O ₄	279	203.0862	159, 181, 116	Veratric acid derivative	A1
25 ^b	7.35	C ₁₆ H ₁₈ O ₉	288, 325	353.0859	<u>191</u> , > <u>179</u> , 203, 135	3-O-(E) caffeoylquinic acid	A2
26 ^b	7.40	C ₁₄ H ₁₈ O ₂ N	287, 323	188.0696*	146, 118, 130, 163	Trans-3-indoleacrylic acid	A2, A1
27 ^b	7.60	C ₂₅ H ₂₀ O ₈	282, 311	447.1125	353, 315, <u>153</u> , <u>137</u>	Dihydroxybenzoic acid hexose-pentose	A2
28 ^b	8.10	C ₁₂ H ₈ O ₄	277	217.0692	133, 191 164, 128	Hydrogenated bergaptol (Bergapten)	A1
	8.10	C ₂₁ H ₂₂ O ₄		356.1353**	302, 339, 340, 182, 326, 229	8-Geranyloxypsoralen	
29 ^b	8.20	C ₂₁ H ₂₂ O ₄	291, 329	357.0812	195, 177, 217, 339	8-Geranyloxypsoralen hydrate	A2
		C ₂₁ H ₂₂ O ₄		341.0859*	305, 261, 179, 163	8-Geranyloxypsoralen	A2
30 ^b	8.40	C ₉ H ₆ O ₄	274	175.0600	131, 129	Esculetin	A1
31 ^b	8.90	C ₁₃ H ₁₂ O ₉	300, 327	311.0396	<u>179</u> , 149	Caftaric acid	A2
32 ^a	9.00	C ₉ H ₇ O ₄	281	179.0336	161, 149, 137	Caffeic acid	A1
	9.00	C ₉ H ₇ O ₄	281	181.0493*	165	Caffeic acid	A1
33 ^b	9.10	C ₉ H ₁₀ O ₄	280	181.0509	137, 121, 109	Veratric acid	A1
34 ^b	9.30	C ₃₉ H ₃₂ O ₁₃	300, 326	707.1815	<u>353</u> , 191	Caffeoylquinic acid dimer	A2
35 ^b	9.70	C ₁₆ H ₁₈ O ₉	300, 326	353.0870	<u>173</u> , > 179, 191, 135	4-O-(E)-caffeoylquinic acid	A2
36 ^b	9.80	C ₉ H ₆ O ₃	300, 326	163.0382*	145, 135	Umbelliferone	A2
37 ^c	9.94	C ₃₇ H ₂₀ O ₁₁	254, 327	639.1176	435, 353, 385, 191, 259, 473	4-O-(E)-caffeoylquinic acid - 3, 5, 7-triacetyl glucoside	A2
	10.00	C ₃₇ H ₂₀ O ₁₁	254, 327	641.1359*	479, 355, 163, 261, 207, 188	4-O-(E)-caffeoylquinic acid - 3, 5, 7-triacetyl glucoside	A2

Table 1 (continued)

Peak no	t _R (min)	Molecular formula	UV λ _{max} (nm)	(M-H) ⁻ /(M+H) ⁺ (m/z)	MS/MS product ions (m/z)	Tentative identification	Sample
38 ^b	10.70	C ₃₅ H ₂₈ O ₁₁	300, 324	623.1575	311, 149, 179, 371, 295, 163	Adduct of 2 individual caftaric acids	A2
39 ^b	10.70	C ₂₇ H ₂₈ O ₅	300, 324	433.1339*	163, 295, 355, 313, 408	Caftaric acid derivative	A2
	11.00	C ₂₇ H ₂₈ O ₅	281, 317	431.1921	349, 305, 172, 311, 216, 395, 179	Caftaric acid derivative	A2
40 ^b	10.90	C ₂₅ H ₂₂ O ₅	284	401.1454	311, 149, 267	Caftaric acid derivative	A2
41 ^b	11.32	C ₂₅ H ₂₄ O ₄	300, 326	387.1648	311, 149	Caftaric acid derivative	A2
42 ^b	11.40	C ₃₅ H ₂₈ O ₁₁	300, 326	623.1621	311, 353, 179, 149	Adduct of 2 caftaric acids	A2
43 ^b	11.50	C ₉ H ₁₀ O ₃	276, 325	165.0559	149, 121, 135	2-(4-hydroxyphenyl) propanoic acid	A1
44 ^b	11.50	C ₉ H ₆ O ₃	276, 325	163.0384*	145, 135	Umbelliferone	A2
45 ^b	11.80	C ₂₁ H ₂₁ O ₁₁	282, 325	449.1075	287, 179, 149, 135, 89	(S)-eriodictyol-6-C-b-D-glucopyranoside	A2
46 ^b	11.80	C ₂₉ H ₂₆ O ₁₃	268, 326	593.1499	515, 191, 353, 145	3,7-diacetyl-3-O-p-coumaroyl-4-O-caf-feoylquinic acid	A2, A1
	11.90	C ₂₉ H ₂₂ O ₁₄	268, 326	595.1661*	516, 451, 163, 339, 521, 309, 499	3,7-diacetyl-3-O-p-coumaroyl-4-O-caf-feoylquinic acid	A2, A1
47 ^b	12.00	C ₂₀ H ₃₄ O ₁₀	310	433.2072	<u>193</u> , <u>325</u> , 131, <u>163</u> , 149	Ferulic acid derivative	A2
48 ^b	12.20	C ₉ H ₁₀ O ₃	280	165.0550	147	Cinnamic acid monohydrate	A1
49 ^b	12.30	C ₁₂ H ₁₈ O ₄	279	225.1150	165, 147	Dimethoxycinnamic acid monohydrate	A1
	12.30	C ₁₂ H ₁₈ O ₄	279	227.1271*	209, 191, 167	Dimethoxycinnamic acid monohydrate	A1
50 ^b	12.30	C ₂₃ H ₁₆ O ₅	282, 322sh	371.0968	249, 225, 173, 149, 311	Hydroxydihydrocaffeoylquinic acid	A2
51 ^b	12.50	C ₁₁ H ₁₁ O ₄	282	206.0817	164, 147, 189	Dimethoxycinnamic acid	A2
52 ^b	12.60	C ₂₁ H ₂₁ O ₁₁	283	449.1162	329, 215, 135	(R)-eriodictyol-6-C-b-D-glucopyranoside	A1
53 ^b	12.70	C ₁₃ H ₇ O ₄	280, 300sh	226.0339	135, 195, 164	Dimethoxycinnamic acid monohydrate	A1
54 ^b	12.90	C ₁₁ H ₁₁ O ₄	280	207.1373*	189, 190	Dimethoxycinnamic acid	A1
55 ^b	13.00	C ₁₇ H ₂₂ O ₁₀	280	385.1134	267, <u>226</u> , 135	Dimethoxycinnamic acid derivative	A2, A1
56 ^b	13.10	C ₁₇ H ₂₀ O ₉	252, 267,	415.1599	<u>367</u> , 385, 247, 311, 269,	Feruloylquinic acid derivative	A2
			282		173, 149		
57 ^b	13.20	C ₇ H ₁₀ O ₆	265	173.0816	149, <u>135</u>	Quinide	A1
58 ^a	13.30	C ₉ H ₈ O ₃	288	163.0399	149	p-Coumaric acid	A2
59 ^c	14.00	C ₁₄ H ₁₂ O ₈	273, 327	245.0944	161, 203	Piceatannol	A2
60 ^b	14.20	C ₁₂ H ₁₈ O ₄	279	209.1365*	191, 167	Dimethoxycinnamic acid monohydrate	A1
61 ^a	14.40	C ₂₇ H ₃₀ O ₁₆	254, 289,	609.1458	300, 431, 341, 293, 179,	Quercetin-3-O-(6-O-rhamnosylglucoside) (rutin)	A2
		331	161, 149				
	14.40	C ₂₇ H ₃₀ O ₁₆	254, 289,	611.1636*	303, 295, 179, 163	Quercetin-3-O-(6-O-rhamnosylglucoside) (rutin)	A2
		331					
62 ^b	14.60	C ₂₇ H ₃₀ O ₁₆	254, 344	609.1457	193, 309, 463, 134, 121, 237, 491	Eriodictyol-7-O-glucuronylrhamnoside	A2
63 ^a	14.60	C ₁₀ H ₁₀ O ₄	275, 300	193.0527	193, 134, 178	Ferulic acid	A1
64 ^b	14.60	C ₁₀ H ₁₂ O ₄	275, 300	197.1167*	177	Dihydro ferulic acid	A1
65 ^b	14.70	C ₂₁ H ₂₀ O ₁₂	254, 348	463.0881	309, 193, 237, 449, <u>287</u>	Eriodictyol-7-O-glucuronide	A2
66 ^b	14.70	C ₁₅ H ₁₀ O ₇	254, 348	303.0488*	153	Quercetin	A2
67 ^b	14.83	C ₁₅ H ₁₀ O ₇	254, 348	303.0500*	153	Quercetin	A2
68 ^b	14.90	C ₂₁ H ₁₈ O ₁₃	255, 287,	477.0670	301, 463, 193, 429	Quercetin-3-O-glucuronide	A2
		352					
	14.90	C ₂₁ H ₁₈ O ₁₃	255, 287,	479.0826*	303, 465	Quercetin-3-O-glucuronide	A2
		352					
69 ^b	15.00	C ₂₁ H ₂₀ O ₁₂	254,	463.0881 (461)	285, 447	Kaempferol-7-O-glucuronide	A2
			351, 414				
70 ^b	15.00	C ₁₅ H ₁₀ O ₇	254,	303.0500*	287, 229, 153	Quercetin	A2
	351, 414						
71 ^b	15.20	C ₂₁ H ₂₁ O ₁₁	267, 363	449.1090	287, 137, 179, 439, 131, 193, 161	(S)-eriodictyol-8-C-b-D-glucopyranoside	A2
72 ^b	15.30	C ₂₁ H ₁₈ O ₁₃	344	477.1071	201, 345, 439, 399, 179	Quercetin-3-O-hexuronide	A2
73 ^b	15.60		300	271.1570	137, 197	Sinapic acid derivative	A1

Table 1 (continued)

Peak no	t _R (min)	Molecular formula	UV λ _{max} (nm)	(M-H) ⁻ /(M+H) ⁺ (m/z)	MS/MS product ions (m/z)	Tentative identification	Sample
74 ^b	15.80	C ₇ H ₁₂ O ₆	291, 311, 332	191.0557	179, 173, 131	Quinic acid	A2
75 ^b	15.90	C ₂₃ H ₂₂ O ₁₃	291, 340	505.0981	353, 191, 463, 301, 447, 417, 491, 179, 159	Quercetin-3-O-acetyl-hexoside	A2
76 ^b	15.90	C ₂₄ H ₂₂ O ₁₅	291, 340	551.1047*	303, 465, 449, 287, 163	Quercetin-3-O-(6 ¹¹ -O-malonyl)-glucoside	A2
77 ^b	16.10	C ₂₅ H ₂₄ O ₁₂	300, 324	515.1204	173, ≥ 179, 353, 191, 135	1,5-di-O-(E) caffeoylquinic acid	A2
78 ^b	16.16	C ₂₅ H ₂₄ O ₁₂	300, 324	515.1216	353, 191, 173, 179, 149, 335	1,5-di-O-(E) caffeoylquinic acid	A2
	16.30	C ₂₅ H ₂₄ O ₁₁	300, 324	499.1239* ^{H2O} 517.1334*	245, 327, 163, 449	1,5-di-O-(E)-caffeoylquinicacid	A2
79 ^b	16.40	C ₂₅ H ₂₄ O ₁₂	300, 327	515.1189	353, ≥ 179, 191, 285, 145	3,5-di-O-(E)-caffeoylquinic acid	A2
	16.50	C ₂₅ H ₂₄ O ₁₁	300, 327	499.1078* ^{H2O} 517.1357*	337, 319, 163, 449, 145, 135	3,5-di-O-(E)-caffeoylquinicacid	A2
80 ^b	16.70	C ₂₁ H ₂₂ O ₁₁	274, 300	453.1975	197, 171, 241, 263, 231, 179	Galloyl salidroside	A1
81 ^b	16.90	C ₇ H ₈ O ₆	266	187.0978	169, 125	Gallic acid monohydrate	A2, A1
82 ^b	17.00	C ₁₅ H ₁₀ O ₆	268, 329, 403	285.0403	179, 243, 183, 221	Kaempferol	A2
83 ^b	17.20	C ₁₅ H ₁₂ O ₆	274	287.1483	229	Dihydrokaempferol	A1
84 ^b	17.30	C ₁₃ H ₁₂ O ₉	330, 403	311.0404	293, 179, 165, 149	Caftaric acid	A2
85 ^b	17.30	C ₂₄ H ₂₃ O ₁₃		519.1121*	295, 303, 163, 401, 447, 287	Isorhamnetin-7-O-(6 ¹¹ -O-acetyl)-glucoside	A2
86 ^b	17.50	C ₇ H ₁₀ O ₆	274	173.1184	127	Quinide	A1
87 ^b	17.60	C ₂₅ H ₂₄ O ₁₂	300, 327	515.1189	173, ≥ 179, 353, 191, 203, 135, 299	3,4-di-O-(E)-caffeoylquinicacid	A2
	17.60	C ₂₅ H ₂₄ O ₁₁	300, 327	499.1237* ^{H2O} 517.1237*	337, 211, 163, 193	3,4-di-O-(E)-caffeoylquinicacid	A2
88 ^b	17.70	C ₁₄ H ₁₂ O ₄	290, 310, 332	243.1243	225, 169, 125, 181, 183	Piceatannol	A1
89 ^b	17.80	C ₂₅ H ₂₄ O ₁₂	300, 327	515.1176	489, 353, 243, 173, 225	4,5-di-O-(E)-caffeoylquinicacid	A2
90 ^b	18.00	C ₁₄ H ₁₂ O ₄	274, 290, 310, 331	243.1231	183, 225, 139	Piceatannol	A2, A1
91 ^b	18.80	C ₂₉ H ₃₄ O ₁₆	255, 269, 295, 350	637.1743	471, 329, 307, 299, 163, 145, 119, 314	Tricin-7-O-rutinoside	A2
	18.80	C ₂₉ H ₃₄ O ₁₆	255, 269, 295, 350	639.1943*	316, 301, 331, 493, 147	Tricin-7-O-rutinoside	A2
92 ^b	19.00	C ₁₄ H ₁₂ O ₄	280	243.1233	171, 225, 159	Piceatannol	A1
93 ^b	19.10	C ₂₃ H ₂₂ O ₁₂	288, 323	491.1187*	343, 285, 161, 471, 243	Kaempferol-3-O-acetylglucoside	A2
	19.30	C ₂₃ H ₂₂ O ₁₂	273, 332, 413	489.1011	285, 179, 221, 343	Kaempferol-3-O-acetylglucoside	A2
94 ^b	19.30	C ₁₅ H ₁₀ O ₆	273, 332, 413	287.0544*	153, 227	Kaempferol	A2
95 ^b	19.40	C ₃₀ H ₃₀ O ₁₈	300, 322, 404	677.1490	533, 285, 489, 179, 135, 299, 515, 353, 225, 161, 269	Kaempferol-3-O-malonylhexoside-7-O-caffeoyl	A2
96 ^b	19.50	C ₁₈ H ₁₇ O ₇	272, 290, 310	343.2144	329, 269, 225, 157	Tricin-4-O-methyl	A1
97 ^b	19.60	C ₂₁ H ₂₀ O ₁₂	328sh	463.1232	301, 329, 149, 285, 173, 225	Quercetin-7-O-hexoside	A2
	19.66	C ₂₁ H ₂₀ O ₁₂	328sh	465.1385*	303, 229	Quercetin-7-O-hexoside	A2
98 ^b	19.80	C ₃₂ H ₂₀ O ₈	285, 327sh	533.1261	285, 173, 135, 151, 301, 353, 475, 463	Kaempferol-3-O-malonylhexoside	A2
99 ^b	19.80	C ₁₅ H ₁₀ O ₆	285, 327sh	287.0547*	229, 153	Kaempferol	A2
100 ^b	20.00	C ₃₀ H ₂₆ O ₁₄	275, 291, 309, 332	609.1254	475, 435, 343, 221, 301, 149, 353, 161, 179, 463	Quercetin-7-O-p-coumaroyl glucoside	A2

Table 1 (continued)

Peak no	t _R (min)	Molecular formula	UV λ _{max} (nm)	(M-H) ⁻ /(M+H) ⁺ (m/z)	MS/MS product ions (m/z)	Tentative identification	Sample
	20.00	C ₃₀ H ₂₆ O ₁₄	275, 291, 309, 332	611.1409*	221, 303, 147, 353, 163, 179, 463	Quercetin-7-O-p-coumaroyl glucoside	A2
101 ^b	20.30	C ₉ H ₁₀ O ₄	291, 310	181.1210	161, 149, 119, 113	Veratric acid	A2
102 ^b	20.30	C ₁₁ H ₁₁ O ₄	291, 310	209.1172*	163, 179	Dimethoxy cinnamic acid	A2
	21.00	C ₁₁ H ₁₁ O ₄	291, 323	207.0661	163, 179	Dimethoxy cinnamic acid	A2
103 ^b	19.90	C ₂₄ H ₂₂ O ₁₅	257, 368	551.1391*	303, 465, 287, 449, 163	Quercetin-3-O-(6 ¹¹ -O-malonyl)-glucoside	A2
104 ^b	21.35	C ₃₂ H ₂₀ O ₈	276, 327, 414	531.1143	285, 349, 442, 161	Kaempferol-3-O-malonylglucoside	A2
105 ^b	21.35	C ₁₅ H ₁₀ O ₆	276, 327, 414	287.0554*	229, 153	Kaempferol	A2
106 ^b	21.60	C ₃₂ H ₂₀ O ₈	274, 327, 413	531.1156	471, 285, 327, 227, 135	Kaempferol-3-C-malonylhexoside	A2
107 ^b	21.60	C ₁₅ H ₁₀ O ₆	274, 327, 413	287.0544*	229, 153	Kaempferol	A2
108 ^b	21.70	C ₃₂ H ₂₀ O ₈	270, 345	533.1284	285, 179	Kaempferol-3-O-malonylhexoside	A2
109 ^b	22.00	C ₃₄ H ₃₀ O ₁₅	300, 328	677.1480	589, 515, 353, 301, 179, 173, 161, 135, 191	3,4,5-Tri-O-caffeoylquinic acid	A2
110 ^b	22.30	C ₃₂ H ₂₀ O ₈	275, 328, 416	531.1135	285, 187, 445, 255, 227	Kaempferol - 3-O-malonylhexoside	A2
	22.30	C ₃₂ H ₂₀ O ₈	275, 328, 416	533.1299*	287, 447	Kaempferol - 3-O-malonylhexoside	A2
111 ^b	22.50	C ₁₅ H ₃₀ O ₁₉	295	513.1383	349, 163, 145, 119, 135, 453,	p-Coumaroyl-feruloylquinic quinide	A2
112 ^b	22.70	C ₂₃ H ₂₂ O ₁₃	290, 341	505.1340	301, 486, 271, 179	Quercetin-3-O-acetylhexoside	A2
	22.70	C ₂₃ H ₂₂ O ₁₃	290, 341	507.1498*	303, 488, 273	Quercetin-3-O-acetylhexoside	A2
113 ^b	22.90	C ₃₀ H ₂₄ O ₁₂	283, 329	575.1409	135, 489, 531, 287, 151	Procyanidin A-type dimer	A2
114 ^b	23.30	C ₃₀ H ₂₄ O ₁₂	282, 329	575.1381	287, 135, 151, 213, 179	Procyanidin A-type dimer	A2
115 ^b	23.40	C ₂₀ H ₂₂ O ₇	270, 290, 309	375.2023	331, 161, 179	Phenylpropenoic acid derivative	A2
116 ^b	23.80	C ₂₃ H ₂₆ O ₁₁	273, 289, 308, 330	519.2427	327, 417, 179, 161, 423, 461	Dihydrocoumarylquinic acid glucoside	A2, A1
117 ^b	23.80	C ₁₈ H ₃₂ O ₅	273	327.2173	171, 183, 229, 211, 291	oxo-dihydroxyoctadecenoic acid	A1
118 ^b	23.80	C ₂₄ H ₂₂ O ₁₅	273	549.1610*	303, 275, 199, 379, 521, 351	Quercetin-3-O-(6 ¹¹ -O-malonyl)-glucoside	A2
119 ^b	23.80	C ₁₆ H ₃₅ NO ₂		275.1994*	195	Amino hexadecanediol	A1
120 ^b	23.90	C ₁₇ H ₁₃ O ₇	238, 289, 308, 348, 376, 395	329.2310	179, 221, 161, 119	Dihydroxyphenylacetic acid -hexoside	A2
121 ^b	23.90	C ₁₈ H ₃₀ O ₃		295.2263*	195, 277, 213, 242	Hydroxylinolenic acid	A1
122 ^b	24.00	C ₁₈ H ₃₄ O ₅	272, 289, 308, 330	329.2325	327, 171, 229, 325	Trihydroxy-octadecadienoic acid	A1
123 ^b	24.00	C ₃₆ H ₆₃ O ₆		591.1699*	563, 520, 298, 380, 254, 192	Hydroxyoctadecadienoic acid dimer	A2
124 ^b	24.10	C ₁₈ H ₃₂ O ₅	274	327.0862*	291, 316	oxo-dihydroxyoctadecenoic acid	A2
125 ^b	24.10	C ₁₅ H ₁₀ O ₇		304.2993**	177, 245	Oxypeucedanin	A1
126 ^b	24.10	C ₁₈ H ₃₄ O ₅		329.2325	311, 213	Trihydroxyoctadecadienoic acid	A1
127 ^b	24.20	C ₁₈ H ₃₀ O ₄		311.2224	171, 236, 309, 293	Dihydroxyoctadecadienoic acid	A1
128 ^b	24.40	C ₁₈ H ₃₀ O ₃		293.2090	275, 171, 183, 235, 265, 285, 135	Hydroxylinolenic acid	A2, A1
129 ^b	24.40	C ₃₆ H ₅₉ O ₄		553.4255*	353, 277, 293, 515, 497	Linolenic acid dimer	A2
130 ^b	24.40	C ₂₂ H ₃₆ O ₄		359.2397*	354, 288, 209	Diacetyl linolenic acid	A1
131 ^b	24.50	C ₁₈ H ₃₂ O ₃		295.2269	275, 171, 116, 97, 263	Hydroxyoctadecadienoic acid	A2
132 ^b	24.50	C ₁₈ H ₃₀ O ₂		278.1743*	233, 203	Linolenic acid	A2, A1
133	24.70	C ₁₈ H ₂₆ N ₂ O ₂		301.2155	201, 283	unknown	A1
134	24.80	C ₂₂ H ₂₇ N ₃ O ₄		398.2325*	321, 203	unknown	A2

Table 1 (continued)

Peak no	t _R (min)	Molecular formula	UV λ _{max} (nm)	(M-H) ⁻ /(M+H) ⁺ (m/z)	MS/MS product ions (m/z)	Tentative identification	Sample
135 ^b	25.20	C ₃₆ H ₆₃ O ₆		593.2771 [*]	513, 469	Hydroxyoctadecadienoic acid dimer	A2
136 ^b	25.60	C ₃₈ H ₆₉ O ₆		621.3065 [*]	561, 460, 533, 505, 102	Methylhydroxyoctadecadienoic acid dimer	A2
137	26.00	C ₄₄ H ₁₄ N ₂ O ₂		601.2636 [*]	520, 227, 345, 159, 135	unknown	A2

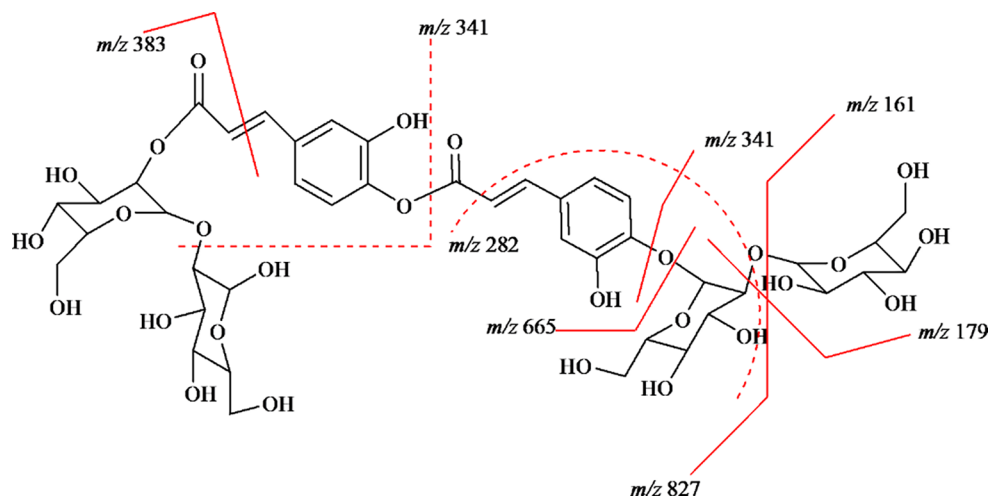
A1: distilled water extracts of *Biden Pilosa* and A2: 70% ethanol extracts of *B. Pilosa*. No asteric = M/z in [M-H]⁻ in the negative ion mode. * = M/z in [M+H]⁺, ^{*H₂O} = [M+H-H₂O]⁺ and ** = [M+NH₄]⁺ in the positive ion mode. ^aIdentified using reference standard, ^bDetermined with the aid of literature using the accurate mass match, reference compound and the number of carbon atoms, ^cNovel compound. Major fragments of the MS/MS product ions are underlined.

base peak ion at m/z 123 [M-H-CO₂]⁻, as well as fragments at m/z 152 [M-H-CH₃]⁻ and m/z 108 [M-H-CO₂-CH₃]⁻. This fragmentation agreed with vanillic acid when compared with the NIST database. Its derivative was identified at peak 73. The compound with peaks of 33 and 104 at Rt 9.10 and 20.30 min, respectively, has [M-H]⁻ at m/z 181. The MS² product-ion analysis of the parent ion provided a fragmentation pattern of the 4-methylated derivative of vanillic acid (veratic acid) in agreement with the literature [41]. Its derivative was identified at peak 24. Peak 21 was identified as a dihydroxy benzoic acid-hexoside, with the [M-H]⁻ ion at m/z 315 and resulting in a fragment at m/z 153 after the loss of 162 and [M-H-hexose-H₂O]⁻ at m/z 135 upon CID [40]. The aglycone ion appeared at Rt 6.10 in peak 20 with a similar product ion as the one in peak 21 and thus was identified as dihydroxy benzoic acid derivative [42]. Peak 81 showed [M-H]⁻; m/z 187, which corresponded to gallic acid monohydrate because MS² fragmentation produces high-intensity peak ions at 169 [M-H]-H₂O]⁻; and m/z 125 [M-H]-H₂O-CO₂]. Its derivative at peak 80 was identified as galloyl solidroside. Peak 120 was identified as dihydroxyphenylacetic acid-hexoside. Compound 43 was identified as 2-(4-hydroxyphenyl) propanoic acid with [M-H]⁻; m/z 165 and MS² fragments m/z 149 [M-H]-OH]⁻, 121 [M-H]-CHO₂]⁻ and 135 [M-H]-OH-CH₃]⁻.

3.3.1.2 Hydroxycinnamic Acids In this study, 46 cinnamic acids were identified with the peaks (10, 14, 15, 17, 18, 21, 22, 23, 24, 25, 31, 32, 33, 34, 35, 37, 38, 39, 40, 41, 42, 46, 47, 48, 49, 50, 51, 53, 54, 55, 56, 58, 60, 63, 64, 73, 77, 78, 79, 84, 87, 89, 102, 103, 111 and 116). Cinnamic acids in their free form were detected, as well as p-coumaric acid (peak 58), caffeic acid (peak 32), ferulic acid or dihydro ferulic acid (peaks 63 or 64), and sinapic acid, which are derivatives of cinnamic acids. In addition, cinnamic acid [cinnamic acid -H]⁻, m/z 147 (peak 48) and its dimethoxy derivative [cinnamic acid -H+60]⁻, identified at peaks 49, 51, 53, 54, 55, 60, and 103, with UV maxima at 291, 310, and 323 nm as in previous work [41]. Sixteen quinic acid (QA) derivatives were identified, including caffeoyl quinic acid (CQA) (6 mono-CQAs; two new ones (37, 46), dimeric

form (34) and other peaks (25, 35, 50), di-CQAs (77, 78, 80, 89, 92), and tri-CQA (112), coumaroyl quinic acid (CoQA) at peaks 17, coumaroyl caffeoyl quinic acid (CoCQA) at peaks 46, feruloylquinic acid (FQA) (56), p-coumaroyl-feruloylquinic acid (CoFQA) (111), and acyl chlorogenic acid (CGA) glycosides (116). Their spectra showed a deprotonated molecular ion at m/z 353 of mono-CQAs and m/z 515 of di-CQA. Fragmentation in the MS/MS produced m/z 191 (QA), which gave a dehydrated quinic acid moiety (m/z 173) and caffeic acid (m/z 179) as a prominent fragment. In addition, their dimeric form shows m/z 707 [2 M-H]⁻ ion with a maximal absorption wavelength of 326 nm. The 4-O-CQA and 3-O-CQA (UV maxima at 300 and 326 nm) were differentiated by the intensity of the characteristic ions of chlorogenic acids. In the former, m/z 173 is the base peak and in the latter, m/z 191 is the base peak [43].

In general, those chlorogenic acids (CGAs) with a greater number of free equatorial hydroxyl groups in quinic acid are more hydrophilic than those with a greater number of free axial hydroxyl groups. On the other hand, the ease of removal of the caffeoyl residue during fragmentation is 1 > 5 > 3 > 4 [44] since hydroxyl groups in the quinic acid are axial in positions 1 and 3, and equatorial in positions 4 and 5 [44]. For di-O-CQAs, the more the additional caffeoyl groups are attached to free equatorial hydroxyl groups (owing to steric interactions), the stronger the retention [45]. That is, the loss of the caffeoyl group (C) is likely to be in the order of 1-C > 5-C > 4-C > 3-C [44, 45]. This enabled peaks 77 and 78, 79, 87, and 89 to be identified as 1,5 di-O-CQA, 3,5 di-O-CQA, 3,4 di-O-CQA, and 4,5 di-O-CQA respectively since the elution order is 1,3-diCQA <<< 1,4-diCQA << 3,4-diCQA < 1,5-diCQA < 3,5-diCQA << 4,5-diCQA [44]. Some of the di-O-CQAs identified above showed the dehydrated protonated molecular ion m/z 499 [M+H-H₂O]⁺ as the most prominent ion in MS² spectra, along with m/z 181 [caffeic acid+H]⁺. It was also observed that their dimeric ion m/z 1033 was present in the MS/MS spectra. This indicates that the original MS ion was m/z 517 [M+H]⁺, in the positive ion mode. The prominent ions for di-CQAs are 4,5-di-CQA has the base peaks, m/z 353, 191, 179, and m/z 173 while

Fig. 3 Proposed fragmentation pattern of**Table 2** The amount of phenolic compounds quantitated from water and 70% ethanol extracts of *Bidens pilosa*

Extracts	Phenolic acids and derivatives mg/L (CAE/ FAE/ CAE)	Flavonols mg/L (RE)	Flavanone mg/L (HE)	Flavan-3-ols mg/L (CE)	Flavone mg/L (RE)	Polyphenols (mg GAE/ g)	Flavonols (mg QE/g)
Water	384.2 ± 3.2	8.5 ± 0.0	N.D.	N.D.	N.D.	18.7 ± 1.5	2.9 ± 0.2
70% ethanol	1855.4 ± 4.8	647.9 ± 3.4	106.4 ± 5.0	21.1 ± 1.5	125.0 ± 32.5	31.6 ± 0.5	18.3 ± 0.1

GAE=Gallic acid equivalents, QE=Quercetin equivalents, CE=Catechin equivalents, CAE=caffeic acid equivalent, FAE=ferulic acid equivalent, RE=rutin equivalent, HE=hesperidin equivalent, CE=catechin equivalent, N.D. = none detected.

3,5-di-CQA has m/z 353 and 179 as base peaks [43, 46]. Peak 50 gave a compound whose fragmentation pattern is similar to that identified by Jaiswal et al. (2014) [47] and thus identified as hydroxydihydrocaffeoylquinic acid. Previous work on chlorogenic profiling of *B. pilosa* has indicated the presence of 4-O-CQA, 3-O-CQA, 4,5-di-CQA, 3,5-di-CQA and tri-CQA [1, 48]. Peak 46 displayed MS m/z 593 giving m/z 515 [CoCQA-H]⁻, 191 [quinat-H]⁻, 353 [CoQA-H]⁻, 145 [Coumaroyl-H-H₂O]⁻, upon CID and thus tentatively identified as 3,7-diacetyl-3-O-p-coumaroyl-4-O-caffeoylquinic acid.

Caftaric acid (CFA) (31, 84) was identified by its parent ion, [M-H]⁻, m/z 311, which fragmented to produce ions at m/z 179 [CA-H]⁻ due to the loss of tartaric acid (TA) residue, m/z 149 [TA-H]⁻ and m/z 135 [FA-CO₂]⁻. This resulted in the decarboxylation of the caffeic acid residue [49]. CFA was initially detected in *B. pilosa* [48]. Derivatives of CFAs were shown at 23, 39, 40, and 41 and individual adducts of 2 CFAs were shown at m/z 623 (peak 38, 42) in agreement with previous work [49]. Chlorogenic acids (CGAs) glycosides showed a typical fragmentation pattern and UV absorbance. All CGAs glycosides were more hydrophilic than their isobaric chlorogenic acids. For instance, mono and diacyl CGAs glycosides were eluted before di- and tri-acyl CGAs, respectively. These glycosides showed fragments that originated from the cinnamoyl glycoside part, e.g., m/z 341 and 323 for caffeoyl glucoside; m/z 355 and 337 for

feruloyl glucoside; m/z 325 and 307 for p-coumaroyl glucoside (peaks 10, 15, and 18 [47, 48]).

Peak 37 from the ethanol extract showed 639 with 435 [M-H-acetylglucose]⁻, 353 [CQA-H]⁻, 385 [2quinat-H+2 H]⁻, 191 [quinat-H]⁻, and 259 [M-H-triacetylglucose-CA-CO₂]⁻, thus, indicating that it is 4-O-(E)-caffeoylquinic acid-3,5,7-triacetyl glucoside. This is a novel compound. Due to the presence of coumaric acid, p-coumaroyl glucoside derivatives could show m/z 163 ([coumaric acid-H]⁻) and MS² fragment m/z 119 ([coumaric acid-CO₂]⁻) [50] and m/z 162 from the glucose conjugation. This led to the identification of novel coumaric acid glucoside derivative peaks (14 and 37). Peak 14 was tentatively described as 1-O-(2¹-O-Coumaryl-1¹¹-O-diglucosyl) caffeoyl-2¹¹¹-O-diglucoside from MS ion m/z 989.3 which, upon MS² fragmentation, ions m/z 179 [CFA-H]⁻, 383, 819, 665, 656, 760, 282, 161 (glucose), 341 [caffeoyl glucoside-H]⁻, 145, 737, 899, 265 were formed. The proposed fragmentation pattern is shown in Fig. 3 below. The other cinnamic acid derivative was observed at peak 47, consisting of a feruloyl (193 Da) moiety with MS² fragments m/z 193 [feruloyl-H]⁻, 325 [feruloyl-H-132]⁻, 163 [feruloyl-H-30]⁻, and 149 [feruloyl-H-CO₂]⁻, and thus considered a ferulic acid derivative.

3.3.2 Characterisation of Flavonoids

3.3.2.1 Dihydroflavonols and Flavonols Flavonols showed strong UV absorption at 258 and 348 nm. Peak 83 was identified to be a dihydroflavonol; dihydrokaempferol associated with initial dehydration of $[M+H]^+$ (NIST) and the other twenty-seven peaks were identified to belong to those of the flavonol compounds (peaks: 61, 66, 67, 69, 70, 72, 75, 76, 82, 83, 85, 93, 94, 95, 97, 98, 99, 100, 103, 104, 105, 106, 107, 108, 110, 112, and 118) in the *B. pilosa* extracts.

Peaks 66, 67, 70, were identified to be those of quercetin; $[quercetin+H]^+$; m/z 303 with common MS² fragments 287 $[quercetin+H-OH]^+$, 229 $[quercetin+H-CHO-OH-CO]^+$ and 153 $[^{1,3}A^+]$, formed through retrocyclization cleavages of the C-ring of the aglycone involving 1 and 3 bonds (bonds 1 and 3 refer to the O—C-2 and C-3—C-4 bonds of the C-ring) [51]. Quercetin aglycone underwent sugar conjugation or esterification to yield rutin (peak 61), consistent with the fragmentation pattern of the standard, quercetin-3-O-hexuronide (peak 72) in negative ion mode, or quercetin-3-O-glucuronide in both negative ion modes; $[M-H]^-$ ion at m/z 477.1 and in the positive ion mode $[M+H]^+$ ion at m/z 479.1. Furthermore, quercetin-3-O-hexoside at peak 97 was formed by the addition of a hexoside (162 Da). Conjugation with malonyl hexoside/glucoside (248 Da) (peaks 76, 103 and 118) and acetyl hexoside (204 Da) (peaks 75 and 112) formed quercetin-3-O-malonyl hexoside, quercetin-3-O-acetyl hexoside, respectively. In addition, simultaneous glucose conjugation and acylation occurred at peak 100 and were identified as quercetin-7-O-p-coumaroyl glucoside from the ethanol extract. These kinds of reactions happened with the kaempferol as the aglycone at peaks 69, 93, 95, 98, 104, 106, 108 and 110, which upon collision inductive dissociation (CID), after losing hexose/glucose or acetyl/ malonyl moieties, the main ions at m/z 285 or 287 were observed, originating from heterolytic cleavage of the O-glycosidic bond. In the peaks; 82, 83, 94, 99, 105 and 107, the CID spectrum of the m/z 285 ion, ($[M-H]^-$ ion) or m/z 287 ($[M+H]^+$ ion) was consistent with kaempferol [42]. In the positive ion mode, the CID with carrier gas could yield MS² fragments; m/z 229 $[kaempferol+H-CH_2OH-CO]^+$ and m/z 153 due to C-ring degradation by fission of the 1,3 bond to produce the RDA fragment $[^{1,3}A^+]$ of the protonated molecule [51]. Peak 85 was identified as isorhamnetin-7-O-(611-O-acetyl) glucoside after acetyl and glucoside residues (206) were added to isorhamnetin aglycone (315Da) with isotopic element combinations.

3.3.2.2 Flavanones Five chromatographic peaks (45, 52, 62, 65, and 71) from *B. pilosa* ethanol and water extracts were considered with flavanone skeletons. Flavanones usually

occur as O-mono- or O-diglycosides derivatives having glucose or rutinose sugars bound to the aglycone hydroxyl group, mostly at C-7. However, peaks 45 and 71, eluting at 11.80 and 15.20 min in the ethanol extract, were identified to be (S) eriodictyol-6-C-b-D-glucopyranoside. Additionally, peak 52 was identified to be (R) eriodictyol-6-C-b-D-glucopyranoside in the water extract of *B. pilosa*. They exhibited a C-linked glucose conjugation at m/z 329 $[M-H-120]$. The aglycone ion at m/z 287 $[eriodictyol-H]^-$, corresponds to eriodictyol associated with characteristic ions m/z 179 $[^{1,4}B^-]$, 149 $[0,2A-H_2O]^-$, 161 $[^{0,4}B^-]$ and 135 $[eriodictyol-H-151(^{1,3}A^-)]^-$, due to retrocyclization fission of the C-ring [51]. The loss of m/z 287 Da from m/z 449.1 yields m/z 162 Da of glucose. Peak 62 of the $[M-H]^-$ ion at m/z 609.1 was identified as eriodictyol-7-O-glucuronylrhamnoside. The ion at m/z 463 was formed after the loss of the rhamnosyl moiety (146Da). The ion at m/z 463 represents eriodictyol-7-O-glucuronide, which is represented at peak 65 [52].

3.3.2.3 Flavones Two flavone peaks were detected and characterised (peaks 91 and 96). In the UV spectrum, maxima at 269, 344, and 258 nm are characteristic of flavones with two hydroxyl groups in ring B. Peak 91 was identified as triclin-7-O-rutinoside in both positive and negative ion mode. The MS² fragments 471 $[M-H-166]^-$, 329 $[M-H-rutinoside]^-$, 307 $[M-H-tricin]^-$, (rutinoside) and m/z 299, 163, 145, 119, and 314 (fragment ions of triclin) were formed. Peak 96 corresponded to that of triclin-4-O-methyl; 329 $[M-H-CH_3]^-$ as major fragment ions compared with database search (Metlin).

3.3.2.4 Flavan-3-ol Peaks 113 and 114 were identified as procyanidin A-type dimer having a sequence of two stereoisomers: catechin and epicatechin flavan-3-ols, respectively. Thus, peak 113 was identified to be catechin-catechin while peak 114 was identified as (epi)catechin-(epi)catechin because the order of hydrophobicity was (-/+)-epicatechin and (-/+)-catechin in the reversed-phase UHPLC. The collision-induced dissociation (CID) of the precursor ions generated fragments like 135 $[epicatechin-152]^-$, 489 $[epicatechin+203]^-$, 531 $[epicatechin+245]^-$, 287 $[M-H-epicatechin]^-$, and 151 $[epicatechin-135]^-$, which were consistent with that of the standard's mass spectra. The fragments m/z 151 and 135 are from RDA fragmentation showing (+)-catechin or (-)-epicatechin. The ion m/z 245 $[catechin-H-44]^-$, loss of CO₂, m/z 205 $[catechin-H-84]^-$, loss of flavonoid

A ring), and m/z 179 ($[M-H-110]^-$, loss of flavonoid B ring) [52].

3.3.3 Stilbenes

Stilbene monomer; piceatannol (m/z 243/245), peaks 11, 59, 88, 90, and 92, was identified with MS² major fragments m/z 225 $[M-H-18]^-$, arising from the loss of a water molecule, and at m/z 201 or 203 $[M-H-42]^-$ and 159 or 161 $[M-H-42-42]^-$ due to successive losses of C₂H₂O (two ketene molecules) [52].

3.3.4 Coumarins and Furanocoumarins

Coumarins and furanocoumarins were detected at peaks 1, 2, 4, 5, 7, 9, 13, 28, 30, 36, 44, and 125. Most of which exhibited UV λ_{\max} at 274 nm, characteristic of coumarin UV absorptions. The $[M-H]^-$ ion at m/z 175.1 (peak 30) with MS² of characteristic ion m/z 131 $[M-H-CO_2]^-$ was identified to be that of the simple coumarin, esculetin. Its derivatives were identified at peaks 1 (its methyl derivative), 5, 7, 13, and that of umbelliferone (hydroxyl coumarin) (peaks 36 and 44). Two hydrogenated furanocoumarin isomers were detected in both extracts (peaks 2 and 28). Peak 2 was tentatively identified as hydrogenated xanthotoxin (hydro psoralen) with an MS² of characteristic ion m/z 192 $[M+H-CO]^+$ and 175 $[M+H-CO_2]^+$. It is the derivative of dimethyl hydroxyl that was identified at peak 4 and peak 29 for that of 8-geranyloxypsoralen. Furthermore, Peak 9 was proposed to be a 5-methoxy-8-hydroxypsoralen dimer with a protonated ion, m/z 465 [53]. The $[M+H]^+$ ion was shown at m/z 232. The fragment at m/z 188 was formed from the RDA cleavage of the furano ring, losing the C₂H₂O⁻ fragment ion. Further loss of the acetylene (C₂H₂⁺) in the lactone ring generated the m/z 166 fragment [53]. Hydrogenated furanocoumarins bergapten, was identified with the MS/MS fragments m/z 133 $[M+H-C_3H_2O^+]$, 191 (formed from RDA cleavage of the furano ring, which lost C₂H₂O⁻). Further loss of the acetylene (C₂H₂⁺) in the lactone ring generated the m/z 164 fragment [53].

3.3.5 Characterisation of Fatty Acids

Next to flavonoids and phenolic acids, fatty acids are the third most abundant class of compounds in *B. pilosa* ethanol and water extracts. There are fourteen known fatty acid peaks (117, 119, 121, 122, 124, 126, 127, 128, 129, 130, 131, 132, 135, and 136) and three unknown fatty acid peaks (133, 134, and 137). Polyunsaturated and hydroxylated fatty acids were the predominant forms. Peak 132 was identified as linoleic acid. This was confirmed by its dimeric form at

peak 129 and its fragmentation pattern, which is similar to previous work [54]. Its hydroxylated form was represented at peaks 121 and 128, while the acetylated derivative conjugate was formed at peak 130. Linoleic acid was found in both extracts of *B. pilosa* analysed in this study. It is an essential fatty acid that possesses anti-inflammatory properties by providing the building blocks for prostaglandins. Several other hydroxylated fatty acids were also detected as major peaks, and they showed extra loss of water molecules [54]. They are known to possess antimicrobial and cytotoxic activities [55]. The polyunsaturated fatty acids included oxo-dihydroxydecanoic acid at peaks of 117 and 124, trihydroxy-fatty acid, and trihydroxyoctadecadienoic acid (peaks of 122 and 126), all found in the water extract. Trihydroxyoctadecanoic acid showed main MS/MS fragments at m/z 311 and 293 due to the subsequent loss of two water molecules and the main fragment at m/z 211 due to the C15\C16 bond cleavage [54]. Additionally, dihydroxy derivatives of octadecanoic acid and dihydroxyoctadecanoic acid were shown at peak 127. Besides, LC-MS revealed several monohydroxy-fatty acid peaks, including hydroxyoctadecanoic acid (peak 131) and its dimeric form, at peaks 123 and 135. It also reveals its methyl dimer derivative, detected at peak 136. Lastly, the saturated fatty acid, amino hexadecanediol, was identified at peak 119, in agreement with previous work [54].

3.3.6 Other Compounds (Carboxylic Acids, Amino Acids or Alkaloids)

The fragmentation of the carboxylic acids occurred through the release of one or two water (18 Da) and carbon dioxide (44 Da) molecules or both (62 Da), and is characterized by the ion fragments $[M-H-18]^-$ and CO₂, $[M-H-44]^-$, or $[M-H-62]^-$. Six peaks were identified as quinic acid or its derivatives (peaks 3, 12, 57, 59, 74, and 86). At m/z 191, quinic acid showed a deprotonated ion; $[quinic-H]^-$. According to Alakolanga et al. (2014) [56], the major characteristic MS² fragment ion at m/z 127 corresponds to the quinic acid residue; $[quinic\ acid-CO-2H_2O]$. Compounds in peaks 6 and 8, were identified as citric acid with major MS² characteristic fragment m/z 173 $[citric-H-18]^-$. Compound 26 was identified as an alkaloid of carboxylic acid. Compound 26 showed a $[M+H]^+$ ion at m/z 188.0696. The MS² fragment at m/z 146 was due to $[M+H-CO_2]^+$ and m/z 118 $[M+H-C_2H_2COOH]^+$ and was tentatively identified as trans-3-indoleacrylic acid which is consistent with the literature [54]. Amino acids were analysed from abundant fragments of the protonated ions and their respective derivatives resulting from either loss of H₂O (-18 Da) yielding their residue mass or loss of (H₂O + CO) to give their immonium

Table 3 LOD and LOQ values calculated for standard phenolic compounds

No	Name	t _R (min)	UV _{λmax} (nm)	m/z (M-H) ⁻	m/z MS/MS	Regression equation	Linear range mg/L	R ²	LOD mg/L	LOQ mg/L
1	Catechin	8.7	278	289	289, 245, 205, 137, 109	y = 1163.4x	3.9–31.3	0.999	1.7	5.8
2	Caffeic acid	9.4	300, 322	179	179, 135	y = 703.7x + 20.9	3.9–31.3	1.000	2.9	9.5
3	Epicatechin	10.8	278	289	289, 245, 205, 137, 109	y = 1553.3x + 938.1	3.9–31.3	0.998	1.3	4.3
4	p-Coumaric acid	11.8	300, 309	163	163, 119	y = 625.1x - 516.0	3.9–31.3	1.000	3.2	10.7
5	Ferulic acid	13.4	300, 322	193	193, 179, 149, 134	y = 487.8x - 57.7	3.9–31.3	0.997	4.1	13.7
6	Rutin	14.5	254, 255, 354	609	609, 301	y = 1155.5x + 205.9	3.9–31.3	0.998	1.7	5.8
7	Hesperidin	17.4	284, 330	609	608, 301	y = 610.4x + 7.9	3.9–31.3	0.994	3.3	11.0
8	Phloridzin	17.9	284	435	435, 273, 167	y = 1308.6x + 1603.3	3.9–15.6	1.000	1.5	5.1

NB: Limit of detection (LOD), Limit of quantification (LOQ).

ions (-46 Da) [54]. Compound 16 was identified as phenylalanine consistent with previous studies [54].

3.3.7 HPLC DAD and UPLC-QTOF-MS Quantitation of Phenolic Compounds

The UV/vis absorptions, capable of distinguishing phenolic subclasses, were considered a starting point for compound quantification. Many aglycone standards have been used in the process, even for the glycosylated forms, especially for O-linked compounds, because their absorption coefficients and the wavelengths of maximum absorption do not change significantly with glycosylation, owing to the fact that glycosidic and alkyl residues are poor chromophores [57]. For C-linked glycosides, however, a new series of conjugated bonds significantly alters the absorption spectra, making the compound's absorption different from the aglycone's [57]. In this study, however, C-linked glycosides were not very prevalent. Based on the qualitative analysis, five chemical markers, namely phenolic acids (caffeic acid (peak 2), ferulic acid (peak 5), and coumaric acid (peak 4)), flavanol (peak 6), dihydrochalcone (peak 8), flavanone (peak 7), and flavano-3-ols (peak 1/3) were selected for simultaneous quantitative determination. They were the most abundant in the extracts. Based on the UV spectrum of the markers, UV detection wavelengths were chosen. The phenolic acids had the strongest UV absorption at 300, 309, and 322 nm, whereas flavanones had UV absorption at 284, 330 nm, flavanols at 254, 255, and 354 nm, dihydrochalcones at 284 nm, and finally flavan-3-ol at 278 nm.

Phenolic compounds were detectable and quantifiable in the aqueous and ethanol extracts of *B. pilosa* (Table 2) and sampled with a high degree of sensitivity, as indicated by their limits of quantification and detection (Table 3). The limits of detection and quantification observed, along with the calculated recoveries, indicate this method's suitability for

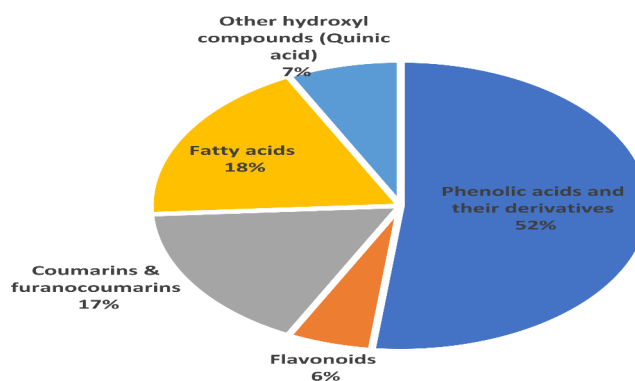


Fig. 4 Mean relative percentile of compound classes identified in the water extract of *Bidens pilosa*. A total of 54 compounds were identified

profiling phenolic compounds from the samples analyzed. The amount has been expressed as caffeic acid, ferulic acid, coumaric acid, rutin catechin, epicatechin, and hesperidin equivalents, and the names of other phenolic compounds are used alternatively and reported in many papers.

3.3.8 Groups of Phytochemicals Identified in the Extracts of *B. pilosa*

A total of 137 metabolites were annotated in the positive and negative ESI modes of both solvent extracts (Figs. 4 and 5). The predominating classes were phenolic acids, flavonoids, fatty acids, coumarins and furanocoumarins, as well as other hydroxyl compounds (Figs. 4 and 5). Among the polyphenolic compounds, phenolic acids and their derivatives were found to be the most abundant compounds in both the water and 70% ethanoic extracts. However, far more phenolic acids, both in bond and free forms, were detected in the ethanol extracts than in the water extract. The phenolic acids determined in the study were 1855.4 ± 4.8 and 384.2 ± 3.2 mg/L CAE/FAE/CoAE in the ethanol extract and water extract, respectively. Flavonoids were the second

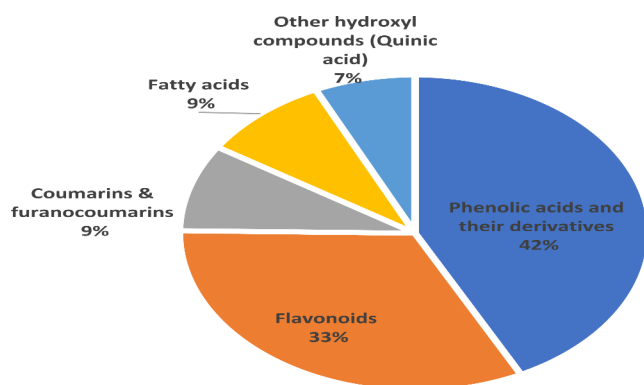


Fig. 5 Mean relative percentile of identified compound classes in the 70% ethanol extract of *Bidens pilosa*. A total of 101 compounds were identified

most abundant compounds detected in the 70% ethanol extract. Given the wide range of uses of *B. pilosa* around the world, the abundance of flavonoids and phenolic acids in the plant might be the basis of the health benefits, biological activities, and other uses of *B. pilosa*.

Phenolic acids, including ester forms of hydroxybenzoic and hydroxycinnamic acids, are major classes identified and are estimated at 52% and 42% in water and 70%-ethanol extracts respectively. However, this percentile was estimated with a total of 54 compounds identified in the water and 101 identified in the ethanol extract. Hydroxybenzoic acids account for 28.57%, while hydroxycinnamic acids make up 71.42% of the phenolic acids in the water extract. The ethanol extract, on the other hand, has 11.62% of hydroxybenzoic acids and 88.37% of hydroxycinnamic acids. Phenolic acids have been reported to have quite a number of beneficiary biological activities, such as anti-diabetic, antiulcer, antioxidant, anticancer, antimicrobial, antiaging, neuroprotection, hepatoprotection, and cardioprotection [58]. The high content of phenolic acids in the extracts of *B. pilosa* could be attributed to its medicinal usage in traditional medicine.

Flavonoids are a class of polyphenolic compounds found primarily in plants and provide health benefits through cell signalling pathways. It could be used as an antioxidant agent, phytoalexin, allopathic compound, and antimicrobial agent [59]. In this study, a total of 3 peaks (6%) of flavonoids in the water extract and 33 peaks (33%) of flavonoids in the 70% ethanol extract, belonging to the main subclasses dihydroflavonol, flavonols, flavanones, flavones, and flavan-3-ol, were tentatively characterized through their characteristic UV spectra.

3.4 Cytotoxicity Using RTCA

The HepG2 (cancerous) and Vero (non-cancerous) cell lines were used to measure the cytotoxic potential of the plant

extracts using two different extraction solvents. The water extract had no significant cytotoxic effect on the HepG2 and Vero cells when compared to the control cells (Figs. 6A and 7A). Interestingly, the lowest and highest concentrations of the water extract stimulated cell growth of the Vero (non-cancerous cells). However, the ethanol extract caused statistically significant toxicity to both cell lines (Figs. 6B and 7B). The two highest concentrations (500 $\mu\text{g}/\text{mL}$ and 1000 $\mu\text{g}/\text{mL}$) were toxic to the HepG2 cells (Fig. 6B), whereas only the highest concentration (1000 $\mu\text{g}/\text{mL}$) of the ethanol extract was cytotoxic to the Vero cells. However, at concentrations ranging from 31.25 $\mu\text{g}/\text{mL}$ –500 $\mu\text{g}/\text{mL}$, the Vero cell lines did not show progressive proliferation (Fig. 7B) compared to the control and 15.6 $\mu\text{g}/\text{mL}$. The lowest concentration (15.6 $\mu\text{g}/\text{mL}$) of the water and ethanol extracts thus stimulated cell growth of the Vero (non-cancerous) cells. An EC_{50} was calculated based on the cytotoxicity caused by the ethanol extract to both cell lines (Table 4, Figs. 6 and 7).

4 Discussion

The use of medicinal plants in various capacities, including disease treatment, pest and weed control in agriculture, and consumption for nutritional benefit, is a common practice among indigenous peoples and those living below the poverty line. The shelf life of the plant product, however, is crucial to its effectiveness because it correlates to the bioactivity of the phytochemicals [60]. Moisture, temperature, and other environmental conditions influence the shelf life of medicinal herbs. According to the study of Müller and Heindl (2006) [61], medicinal plant specimens are best stored at a final moisture content (MC) not higher than 13%, relative humidity of less than 70%, and at 25 °C to reduce the development of microorganisms such as bacteria, fungi, and yeasts, as well as pest infestation. In this study, the moisture content of *B. pilosa* was found to be 5.14% when air-dried at room temperature. This indicates that the plant could be air-dried until a constant mass to attain a safe condition, especially if intended for consumption as a herbal remedy or diet purposes. The potency of the phytochemicals will also be at its optimal under the conditions stated above.

Plants are known to contain different metabolites, including natural antioxidants, that help to protect and preserve their metabolism as well as their physical integrity. A number of plant phytochemicals with antioxidant characteristics have been identified, with examples including hydrosoluble antioxidants such as phenolics, flavonoids, anthocyanins, stilbene, and lignan, as well as liposoluble antioxidants such as β -carotene, α -carotene, lycopene, lutein, zeaxanthin, minerals, and vitamins [62]. Recent studies suggest that the

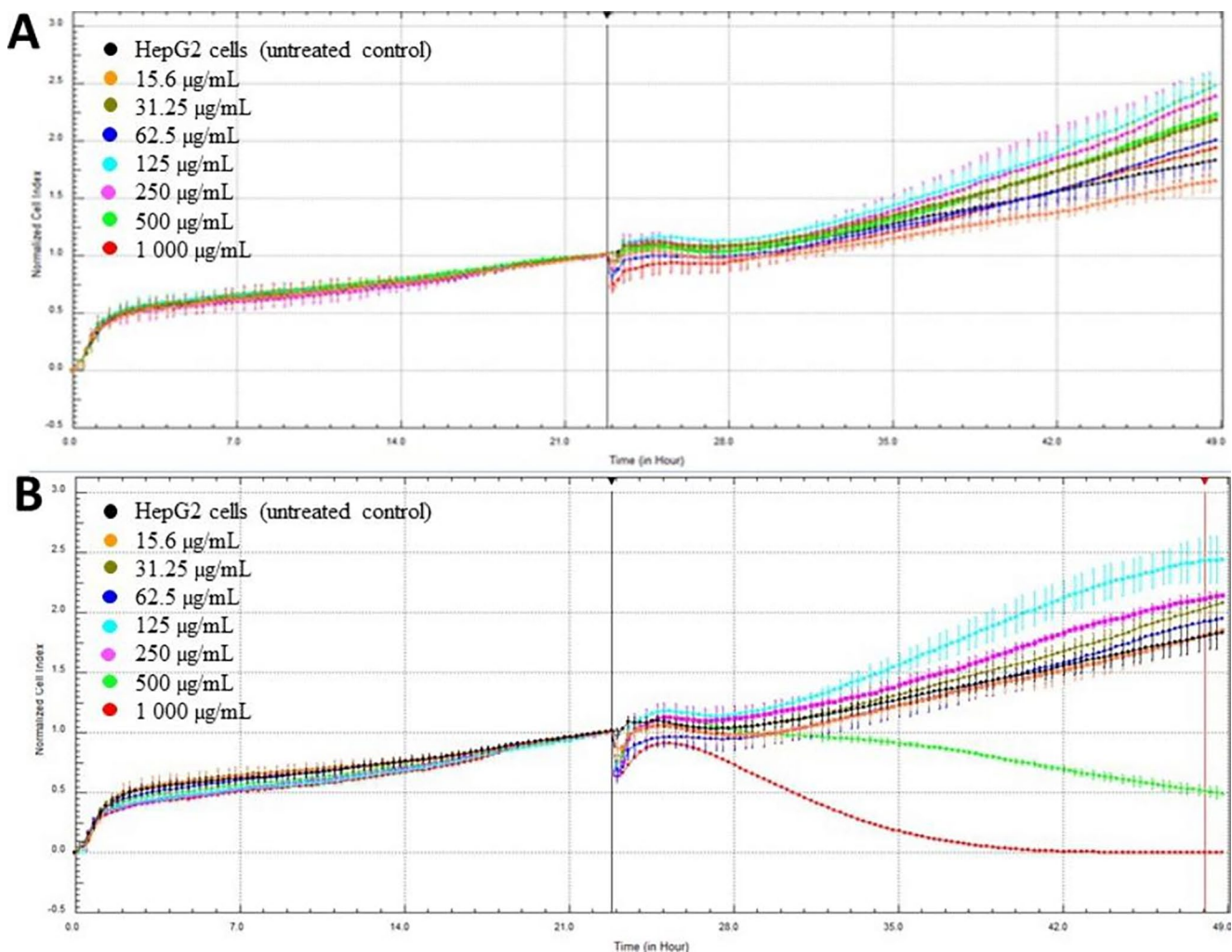


Fig. 6 Growth curves (cell index) of HepG2 cells after exposure to a concentration range of *Bidens pilosa* extracts (A) water and (B) ethanol extracts. The normalisation time point was 23 h. Error bars represent standard deviation

overproduction of reactive nitrogen species (RNS) and reactive oxygen species (ROS), as well as hydroxyl radicals, nitrosonium, hydrogen peroxide, nitroxyl anion, peroxy-nitrite, and superoxide, could be the leading causes of oxidative stress. This could result in other pathogenic processes, such as DNA damage and inflammatory diseases [63]. From this point of view, compounds with molecules capable of scavenging or reducing high ROS/RNS and free radicals would be of health benefit in managing illnesses such as cancer, diabetes, heart disease, neurodegenerative diseases, and ageing [58]. *Bidens pilosa* could offer these benefits because of its high polyphenols (an antioxidant) ranging from 15.66 to 20.19 mg GAE/g in the water extract and from 30.86 to 32.52 mg GAE/g for the ethanol extract, with a subclass of 54% and 42% phenolic acid, respectively. The total amount of total polyphenol estimated in this study is similar to the study of Cortés-Rojas et al. (2013) [64] who estimated the total polyphenol content of *B. pilosa* to be about 20 mg

GAE/g (leaves/flower samples), 18 mg GAE/g (stems samples) and less than 10 mg GAE/g (root samples) for ethanol using water extraction solvent (62.7%, v/v) and ethanol: water (70%, v/v) for samples collected at multiple locations in Brazil [64]. Wu et al. (2013) [65], however, reported a lesser amount of total phenolic (26.84 to 272.35 µg GAEs/mg) and flavonoid content (5.65 to 524.51 µg PEs/mg) in a 75% ethanol solvent extract of *B. pilosa* using a spectrophotometry method. Singh et al. (2017) [66], also reported the phenolic content of *B. pilosa* to be 72 µg GAE/mg dry mass and total flavonoids of 123.3 µg QE/mg dry mass. This might be a result of the differences in the geographical locations, weather exposures of the plants, and analytical equipment.

Spectrophotometric methods revealed the flavonol content, a subclass of flavonoids is 2.92 mg QE/g in the water extract and 18.31 mg QE/g in the ethanol extract in the present study. According to the developed UPLC-ESI-QTOF-MS

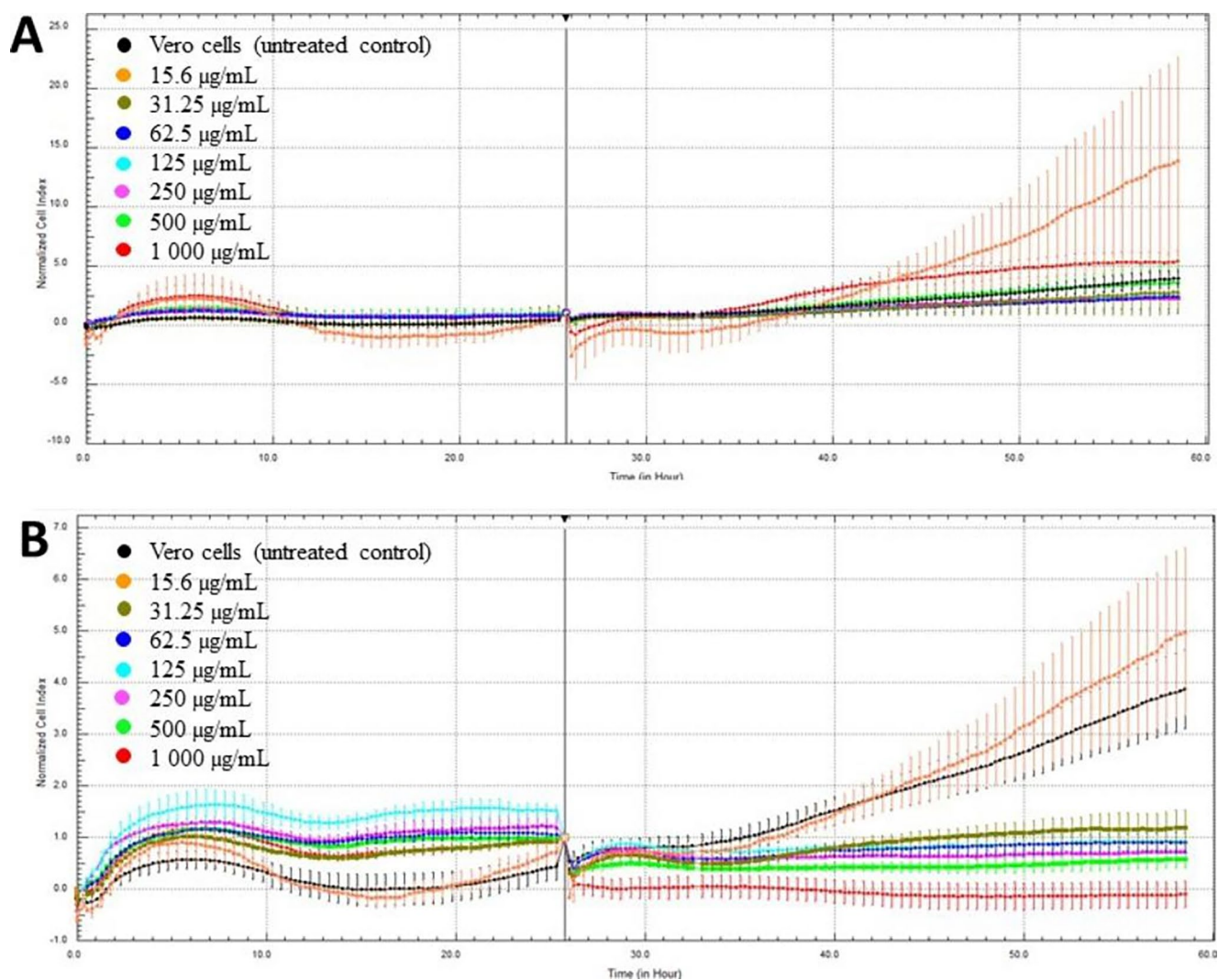


Fig. 7 Growth curves (cell index) of Vero cells after exposure to a concentration range of *Bidens pilosa* (A) water and (B) ethanol extracts. The normalisation time point was 26 h. Error bars represent standard deviation

Table 4 Effective concentrations (EC_{50}) of the plant extracts using 2 different solvents: water and ethanol using the HepG2 and Vero cells

HepG2 cells			
	EC_{50} ($\mu\text{g/mL}$)	Cellular response	R^2
<i>Bidens pilosa</i> (water)	No value	Non-cytotoxic	
<i>Bidens pilosa</i> (70% ethanol)	1.7×10^{-5}	Cytotoxic*	0.973
Vero cells			
	EC_{50} ($\mu\text{g/mL}$)	Cellular response	R^2
<i>Bidens pilosa</i> (water)	No value	Non-cytotoxic	
<i>Bidens pilosa</i> (70% ethanol)	1.7×10^{-5}	Cytotoxic*	0.8370

EC: effective concentration, R^2 : coefficient of determination

methods, flavonols were not detected in the water extracts, but other subgroups of flavonoids such as dihydroflavonol, flavanones, and flavones were found at 33% each. However, the flavonol in the ethanol extract was 78.78% of the flavonoid content. Flavonoids and phenols are important components of diets and medications due to their inherent health-promoting properties, which include anti-oxidative, anti-inflammatory, anti-mutagenic, anti-carcinogenic, anti-microbial, and larvicidal properties [59]. *Bidens pilosa* has been reported to be used in the treatment of various diseases, including hyperglycemia [8], malaria [9], tumours [10], and inflammation [12], which could be linked to the high possession of flavonoids and phenols. The antioxidant activities of the ethanol extracts are higher compared to the water extract. According to this study, the peaks in the ethanol extract are higher than in the water extract, with a total of 101 peaks belonging to four main classes: phenolic

acids, flavonoids, fatty acids, coumarins and furanocoumarins, as well as other hydroxyl compounds. The number of flavonoids was relatively high, about six-fold more than that which is present in the water extract. The antioxidant activity is both the individual and joint effect of the metabolites in the plant sample. Our study reveals the antioxidant activities of the ethanol extracts are higher, indicating a higher potency, and this correlates with the number of peaks or phytochemicals. The antioxidant capabilities of different solvent extractions of *Severinia buxifolia* were studied by Truong et al. (2019) [67], and water extract was shown to have the least activity, while ethanol was found to be the second most active, after methanol.

Other classes of compounds with health benefits such as coumarins and related compounds were also annotated in the extract of *B. pilosa*. These compounds have become relevant in recent years due to their various biological activities. Coumarins and related compounds in their natural or synthetic forms have been reported to be used as antibiotics [68], anti-inflammatory and antinociceptive [69], photochemotherapy and anti-HIV therapy [70], cancer and antioxidant agents [71]. Aside from their medical use, coumarins are also utilized in various industries, such as the cosmetic, and agrochemical industries, as optical brightening agents, laser dyes and dispersed fluorescent [70]. This study suggests that *B. pilosa* could serve as a natural source of coumarins and furanocoumarins, with water solvent being a more effective extractant than ethanol.

The cytotoxicity of the extract followed a similar trend to the results of other assays in this study. Cytotoxicity is a non-specific endpoint of toxicity and can be applied as an early warning sign since it is a reflection of the toxic response elicited by chemicals present in mixtures as in the case of plant extracts [72]. Cell death is reflected by a slowdown in metabolic activity [34] and can be measured using various viability assays. In this study, the cytotoxic potential of *B. pilosa* water and ethanol extracts were assessed using different cell lines: HepG2 and Vero. Concentration-dependent cytotoxicity was observed after exposure to the ethanol extracts. The high concentrations of the ethanol extracts were cytotoxic to both cell lines compared to the water extracts rather than promoted cell proliferation – specifically of the Vero (non-cancerous) cells. The cytotoxicity caused by the ethanol extract could be attributed to more phytochemicals present in the ethanol extract, particularly flavonoids when compared to the water extract. An extensive investigation has been carried out with flavonoids against various cancer cell lines such as breast, prostate, liver, lung, melanoma, pancreas, and stomach., which proved effective against cancer cells, making flavonoids an anticancer agent. It has, however, been used as a chemoprevention agent as well as a cancer treatment agent [73]. The same

observation was noted in the current study, where the flavonoid-rich (ethanol) extract was responsible for killing the HepG2 cancerous cells—but the Vero non-cancerous cells were also killed after exposure to the ethanol extract. This highlights the need to include different types of cell lines for cytotoxicity assessment, especially in the application to test chemicals for their anticancer abilities to ensure that non-cancerous cells are not negatively affected. Phenolic acids, for both solvents of extraction, are the highest annotated class of compound. According to Saibabu et al. (2015) [58], phenolic acids help in disease prevention and therapy through cell growth promotion using their antioxidants and anti-inflammatory properties [58] which is contrary to the activity of flavonoids, particularly against cancerous cells. This implies that flavonoids do not promote cell proliferation, unlike phenolic acids. The simulated growth observed in the Vero cells after exposure to both types of extracts (water and ethanol), could be ascribed to the presence of phenolic compounds in the extracts. Although this might be the case for the Vero cells, in contrast, the HepG2 cells did not show simulated growth patterns. This observation in differences in vulnerabilities between the types of cells is due to genetic differences between the two cell lines [74].

The EC_{50} values determined in this study using the xCELLigence technology are substantially lower compared to previous studies where cytotoxicity of *B. pilosa* methanolic extracts was determined using the MTT assay with HepG2 cell lines [66]. This difference could be attributed to the increased sensitivity of the xCELLigence compared to the MTT assay or the use of different solvents, i.e., we used ethanol instead of methanol. In contrast to the absence of EC_{50} values (no cytotoxicity observed) for the water extracts in the current study, Abdel-Ghany et al. (2016) [75] published EC_{50} of 1000 $\mu\text{g/ml}$ after exposure of aqueous extracts of *B. pilosa* to primary cell cultures (rat hepatocytes). These authors used primary cell cultures (short life span) in contrast to the immortal cell lines used in the current study. One should, however, keep in mind that the cells are cultured in tissue culture dishes without the benefit of an immune system and are merely indicative of toxicity potential. The results indicate the potential toxicity exhibited by the ethanol extracts. These effects might be different when whole organisms are used or exposed due to their defence mechanisms.

5 Conclusion

This study is a comprehensive secondary metabolite profiling and cytotoxicity that aims to provide chemical-based evidence for the health benefits of *B. Pilosa*. The analytical methods used were HPLC-DAD and

UHPLC-ESI-Q-TOF-MS, which enabled the separation as well as annotation of 137 secondary metabolites, mainly predominated by phenolic acids, flavonoids, and fatty acids. The plant (ethanol extract) is cytotoxic but not poisonous, as no potentially poisonous compound was identified. These findings provide further evidence for the value of the plant as a source of functional phytoconstituents and also explain the impact of solvents of extraction (ethanol and water) on the bioactivity of the plant.

Acknowledgements The authors would like to thank Hein Hendrik Smith for his assistance in locating and collecting plant samples (*Bidens pilosa*).

Funding Statement The authors do not receive any funding from an external source. Open access funding provided by North-West University.

Availability of Data and Material All data generated or analysed during this study are included in this article.

Declarations

Competing interests The authors declare that there is no conflict of interest associated with this publication. All authors have read and agreed to the publication of the manuscript.

Open Access This article is licensed under a Creative Commons Attribution 4.0 International License, which permits use, sharing, adaptation, distribution and reproduction in any medium or format, as long as you give appropriate credit to the original author(s) and the source, provide a link to the Creative Commons licence, and indicate if changes were made. The images or other third party material in this article are included in the article's Creative Commons licence, unless indicated otherwise in a credit line to the material. If material is not included in the article's Creative Commons licence and your intended use is not permitted by statutory regulation or exceeds the permitted use, you will need to obtain permission directly from the copyright holder. To view a copy of this licence, visit <http://creativecommons.org/licenses/by/4.0/>.

References

- Chiang YM, Chuang DY, Wang SY, Kuo YH, Tsai PW, Shyur LF (2004) Metabolite Profiling and Chemopreventive Bioactivity of Plant extracts from *Bidens Pilosa*. *J Ethnopharmacol* 95:409–419. <https://doi.org/10.1016/j.jep.2004.08.010>
- Yang W, Botanical (2014) Pharmacological, Phytochemical, and Toxicological Aspects of the Antidiabetic Plant *Bidens Pilosa* L. Evidence-Based Complementary and Alternative Medicine 1–14
- Li BL, Xie JD, Xie FD, Li HY, Hu JJ, Li QR, Liang HJ, Ao ZY, Fan YW, Zhang WJ et al (2021) Polyacetylenes from *Bidens Pilosa* Linn., Promising Insecticides with anti-inflammatory Effects on HaCaT cells. *Ind Crops Prod* 171:113929. <https://doi.org/10.1016/j.indcrop.2021.113929>
- Sun Y bing, Zhou Q, Liu W (2009) ; An, J.; Xu, Z.Q.; Wang, L. Joint Effects of Arsenic and Cadmium on Plant Growth and Metal Bioaccumulation: A Potential Cd-Hyperaccumulator and As-Excluder *Bidens Pilosa* L. *J Hazard Mater* 165, 1023–1028, doi:<https://doi.org/10.1016/j.jhazmat.2008.10.097>
- Yan A, Wang Y, Tan SN, Mohd Yusof ML, Ghosh S, Chen Z (2020) Phytoremediation: a Promising Approach for Revegetation of Heavy Metal-Polluted Land. *Front Plant Sci* 11:359. <https://doi.org/10.3389/FPLS.2020.00359/BIBTEX>
- Xuan TD, Shinkichi T, Khanh TD, Chung IM (2005) Biological control of weeds and plant pathogens in Paddy Rice by exploiting Plant Allelopathy: an overview. *Crop Prot* 24:197–206. <https://doi.org/10.1016/j.cropro.2004.08.004>
- Bartolome AP, Villaseñor IM, Yang WC, Bidens Pilosa L (Asteraceae) (eds) (2013) : Botanical Properties, Traditional Uses, Phytochemistry, and Pharmacology. *Evidence-based Complementary and Alternative Medicine* 2013, 1–51, doi:<https://doi.org/10.1155/2013/340215>
- Hsu YJ, Lee TH, Chang CLT, Huang YT, Yang WC (2009) Anti-hyperglycemic Effects and mechanism of *Bidens Pilosa* Water Extract. *J Ethnopharmacol* 122:379–383. <https://doi.org/10.1016/j.jep.2008.12.027>
- Andrade-Neto VF, Brandão MGL, Oliveira FQ, Casali VWD, Njaine B, Zalis MG, Oliveira LA, Krettli AU (2004) Antimalarial activity of *Bidens Pilosa* L. (Asteraceae) ethanol extracts from wild plants collected in various localities or plants cultivated in Humus Soil. *Phytother Res* 18:634–639. <https://doi.org/10.1002/ptr.1510>
- Kwiecinski MR, Felipe KB, Schoenfelder T, de Lemos Wiese LP, Rossi MH, Gonçalez E, Felicio JD arc, Filho DW, Pedrosa RC (2008) Study of the Antitumor Potential of *Bidens Pilosa* (Asteraceae) Used in Brazilian Folk Medicine. *J Ethnopharmacol* 117, 69–75, doi:<https://doi.org/10.1016/j.jep.2008.01.017>
- Khan MR, Kihara M, Omoloso AD (2001) Anti-microbial activity of *Bidens Pilosa*, *Bischofia Javanica*, *Elmerillia* Papua and *Sigesbekia Orientalis*. *Fitoterapia* 72:662–665. [https://doi.org/10.1016/S0367-326X\(01\)00261-1](https://doi.org/10.1016/S0367-326X(01)00261-1)
- Hong M, Fan X, Liang S, Xiang W, Chen L, Yang Y, Deng Y, Yang M (2020) Total flavonoids of *Bidens Pilosa* ameliorates Bone Destruction in Collagen-Induced Arthritis. *Planta Med*. <https://doi.org/10.1055/a-1352-5124>
- Salazar MJ, Wannaz ED, Blanco A, Miranda Pazcel EM, Pignata ML (2021) Pb Tolerance and Accumulation Capabilities of *Bidens Pilosa* L. growing in Polluted Soils depend on the history of exposure. *Chemosphere* 269:128732. <https://doi.org/10.1016/J.CHEMOSPHERE.2020.128732>
- Ahmed S, Abdel-Aziz S, Taha A, Elhefny A (2021) Insecticidal Effects of two plant extracts of (*Bidens Pilosa* and *Rumex Dentatus*) and neem oil against certain stored grains insects. *Egypt Acad J Biol Sci F Toxicol Pest Control* 13:149–158. <https://doi.org/10.21608/eajbsf.2021.153352>
- Tembo Y, Mkindi AG, Mkenda PA, Mpumi N, Mwanauta R, Stevenson PC, Ndakidemi PA, Belmain SR (2018) Pesticidal plant extracts improve yield and reduce insect pests on legume crops without harming beneficial arthropods. *Front Plant Sci* 9:1425. <https://doi.org/10.3389/fpls.2018.01425>
- Falowo AB, Mukumbo FE, Muchenje V (2019) Phytochemical constituents and antioxidant activity of *Artemisia Afra* and *Bidens Pilosa* essential oil in ground pork. *J Essent Oil-Bearing Plants* 22:176–186. <https://doi.org/10.1080/0972060X.2019.1574212>
- Mersie W, Alemayehu L, Strathie L, McConnachie A, Terefe S, Negeri M, Zewdie K (2019) Host range evaluation of the Leaf-Feeding Beetle, *Zygogramma Bicolorata* and the stem-boring Weevil, *Listronotus Setosipennis* demonstrates their suitability for Biological Control of the Invasive Weed, *Parthenium Hysterophorus* in Ethiopia. *Biocontrol Sci Technol* 29:217–229. <https://doi.org/10.1080/09583157.2018.1545220>
- Bajracharya ASR, Thapa RB, Pradhan SB, Ranjit JD (2020) Evaluation of host-specificity of *Zygogramma Bicolorata* Pallister

- (Coleoptera: Chrysomelidae) for the Biological Control of Parthenium Hysterophorus L.(Asteraceae: Heliantheae) in Nepal. *J Agric Nat Resour* 4:29–41
19. Taba S, Ashikaga K, Oohama T, Ajitomi A, Kiyuna C, Kinjo M, Sekine KT (2020) Bidens Pilosa Extract Effects on Pine Wilt: Causal Agents and their natural enemies. *For Sci* 66:284–290. <https://doi.org/10.1093/forsci/fxz076>
 20. Poonpaiboonpipat T, Poolkum S (2019) Utilization of Bidens Pilosa Var. Radiata (Sch. Bip.) Sherff Integrated with Water Irrigation for Paddy Weed Control and Rice Yield production. *Weed Biol Manag* 19:31–38. <https://doi.org/10.1111/WBM.12173>
 21. Lans C, Sant C, Georges K (2019) Ethnoremedies Used for Horses in British Columbia and Trinidad and Tobago. In *Ethnoveterinary Medicine: Present and Future Concepts*; Springer International Publishing, ; pp. 57–71 ISBN 9783030322700
 22. Chang CLT, Chung CY, Kuo CH, Kuo TF, Yang CW, Yang WC (2016) Beneficial effect of Bidens Pilosa on Body Weight Gain, Food Conversion ratio, gut Bacteria and coccidiosis in chickens. *PLoS ONE* 11:e0146141. <https://doi.org/10.1371/journal.pone.0146141>
 23. Yuan LP, Chen FH, Ling L, Dou PF, Bo H, Zhong MM, Xia LJ (2008) Protective Effects of total flavonoids of Bidens Pilosa L. (TFB) on Animal Liver Injury and Liver Fibrosis. *J Ethnopharmacol* 116:539–546. <https://doi.org/10.1016/J.JEP.2008.01.010>
 24. Dimo T, Azay J, Tan PV, Pellecuer J, Cros G, Bopelet M, Serano JJ (2001) Effects of the Aqueous and Methylene Chloride extracts of Bidens Pilosa Leaf on Fructose-Hypertensive rats. *J Ethnopharmacol* 76:215–221. [https://doi.org/10.1016/S0378-8741\(01\)00229-X](https://doi.org/10.1016/S0378-8741(01)00229-X)
 25. Smith HH, Idris OA, Maboeta MS (2021) Global Trends of Green Pesticide Research from 1994 to 2019: a bibliometric analysis. *J Toxicol* 2021. <https://doi.org/10.1155/2021/6637516>
 26. Thirumurugan D, Cholarajan A, Raja SSS, Vijayakumar R (2018) An introductory chapter: secondary metabolites. *Secondary Metabolites - Sources and Applications* 1–21. <https://doi.org/10.5772/INTECHOPEN.79766>
 27. Daniels CW, Rautenbach F, Marnewick JL, Valentine AJ, Babajide OJ, Mabusela WT (2015) Environmental stress effect on the phytochemistry and antioxidant activity of a south african bulbous geophyte, Gethyllis Multifolia L. *Bolus*. *South Afr J Bot* 96:29–36. <https://doi.org/10.1016/j.sajb.2014.10.004>
 28. Idris OA, Wintola OA, Afolayan AJ (2017) Phytochemical and antioxidant activities of Rumex Crispus L. in treatment of gastrointestinal Helminths in Eastern Cape Province, South Africa. *Asian Pac J Trop Biomed* 7:1071–1078. <https://doi.org/10.1016/j.apjtb.2017.10.008>
 29. Re R, Pellegrini N, Proteggente A, Pannala A, Yang M, Rice-Evans C (1999) Antioxidant activity applying an Improved ABTS Radical Cation Decolorization Assay. *Free Radic Biol Med* 26:1231–1237. [https://doi.org/10.1016/S0891-5849\(98\)00315-3](https://doi.org/10.1016/S0891-5849(98)00315-3)
 30. Jimoh MO, Afolayan AJ, Lewu FB (2019) Antioxidant and phytochemical activities of Amaranthus Caudatus L. Harvested from different soils at various growth stages. *Sci Rep* 9:12965. <https://doi.org/10.1038/s41598-019-49276-w>
 31. Zeb AA, Reversed Phase (2015) HPLC-DAD method for the determination of Phenolic Compounds in Plant Leaves. *Anal Methods* 7:7753–7757. <https://doi.org/10.1039/C5AY01402F>
 32. Zubarev RA, Makarov A (2013) Orbitrap Mass Spectrometry. *Anal Chem* 85:5288–5296. <https://doi.org/10.1021/AC4001223>
 33. Branch SK (2005) Guidelines from the International Conference on Harmonisation (ICH). *J Pharm Biomed Anal* 38, 798–805, doi:<https://doi.org/10.1016/J.JPBA.2005.02.037>
 34. Belaid A, Methneni N, Nasri E, Bchir S, Anthonissen R, Verschaeve L, le Tilly V, lo Turco V, di Bella G, Mansour H et al (2021) ben;. Endocrine Disruption, Cytotoxicity and Genotoxicity of an Organophosphorus Insecticide. *Sustainability* 2021, Vol. 13, Page 11512 13, 11512, doi:<https://doi.org/10.3390/SU132011512>
 35. Taft DR, Drug Excretion (2009) *Pharmacology* 175–199, doi:<https://doi.org/10.1016/B978-0-12-369521-5.00009-9>
 36. Prinsloo S, Rialet P, Carlos CB (2013) A cell viability assay to determine the cytotoxic Effects of Water contaminated by microbes. *S Afr J Sci* 7:1–4
 37. Mišek M, Marcinčáková D, Legáth JP, Content (2019) Antioxidant activity, and cytotoxicity Assessment of Taraxacum Officinale extracts prepared through the micelle-mediated extraction method. *Molecules* 2019 24:1025. <https://doi.org/10.3390/MOLECULES24061025>
 38. Stefanowicz-Hajduk J, Ochocka JR (2020) Real-time cell analysis system in cytotoxicity applications: usefulness and comparison with tetrazolium salt assays. *Toxicol Rep* 7:335–344. <https://doi.org/10.1016/J.TOXREP.2020.02.002>
 39. Urcan E, Haertel U, Styllou M, Hickel R, Scherthan H, Reichl FX (2010) Real-time XCELLigence impedance analysis of the cytotoxicity of Dental Composite Components on Human Gingival fibroblasts. *Dent Mater* 26:51–58. <https://doi.org/10.1016/J.DENTAL.2009.08.007>
 40. Fu S, Arráez-Roman D, Segura-Carretero A, Menéndez JA, Menéndez-Gutiérrez MP, Micol V, Fernández-Gutiérrez A (2010) Qualitative screening of Phenolic Compounds in Olive Leaf extracts by Hyphenated Liquid Chromatography and preliminary evaluation of cytotoxic activity against human breast Cancer cells. *Anal Bioanal Chem* 397:643–654. <https://doi.org/10.1007/S00216-010-3604-0/FIGURES/8>
 41. Moqbel H, El Hawary SSED, Sokkar NM, El-Naggar EMB, El Boghdady N, El Halawany AM, HPLC-ESI-MS/MS (2018) Characterization of phenolics in Prunus Amygdalus, Cultivar “Umm Alfahm” and its antioxidant and Hepatoprotective Activity. *J Food Meas Charact* 12:808–819. <https://doi.org/10.1007/S11694-017-9695-Y/FIGURES/4>
 42. Gouveia SC, Castilho PC (2010) Characterization of Phenolic Compounds in Helichrysum Melaleucum by High-Performance Liquid Chromatography with on-line Ultraviolet and Mass Spectrometry Detection. *Rapid Commun Mass Spectrom* 24:1851–1868. <https://doi.org/10.1002/RCM.4585>
 43. Crozier A, Jaganath IB, Clifford MN (2009) Dietary phenolics: Chemistry, Bioavailability and Effects on Health. *Nat Prod Rep* 26:1001–1043. <https://doi.org/10.1039/B802662A>
 44. Clifford MN, Knight S, Kuhnert N (2005) Discriminating between the six Isomers of Dicafeoylquinic Acid by LC-MSn. *J Agric Food Chem* 53:3821–3832. <https://doi.org/10.1021/JF050046H/ASSET/IMAGES/LARGE/JF050046HF00014.JPG>
 45. Liao SG, Zhang LJ, Li CB, Lan YY, Wang AM, Huang Y, Zhen L, Fu XZ, Zhou W, Qi XL et al (2010) Rapid Screening and Identification of Caffeic Acid and its Esters in Erigeron Breviscapus by Ultra-Performance Liquid Chromatography/Tandem Mass Spectrometry. *Rapid Commun Mass Spectrom* 24:2533–2541. <https://doi.org/10.1002/RCM.4662>
 46. Schram K, Miketova P, Slanina J, Humpa O, Taborska E (2004) Mass Spectrometry of 1,3- and 1,5-Dicafeoylquinic acids. *J Mass Spectrom* 39:384–395. <https://doi.org/10.1002/JMS.600>
 47. Jaiswal R, Müller H, Müller A, Karar MGE, Kuhnert N (2014) Identification and characterization of chlorogenic acids, Chlorogenic Acid Glycosides and Flavonoids from Lonicera Henryi L. (Caprifoliaceae) Leaves by LC–MSn. *Phytochemistry* 108:252–263. <https://doi.org/10.1016/J.PHYTOCHEM.2014.08.023>
 48. Ramabulana AT, Steenkamp P, Madala N, Dubery IA (2020) Profiling of chlorogenic acids from Bidens Pilosa and differentiation of closely related positional isomers with the aid of UHPLC-QTOF-MS/MS-Based In-Source Collision-Induced dissociation. *Metabolites* 2020 10. <https://doi.org/10.3390/METABO10050178>. 10

49. Carazzone C, Mascherpa D, Gazzani G, Papetti A (2013) Identification of Phenolic Constituents in Red Chicory Salads (*Cichorium Intybus*) by high-performance liquid chromatography with diode array detection and Electrospray Ionisation Tandem Mass Spectrometry. *Food Chem* 138:1062–1071. <https://doi.org/10.1016/J.FOODCHEM.2012.11.060>
50. Hokkanen J, Mattila S, Jaakola L, Pirttilä AM, Tolonen A (2009) Identification of Phenolic Compounds from Lingonberry (*Vaccinium Vitis-Idaea* L.), Bilberry (*Vaccinium Myrtillus* L.) and hybrid bilberry (*Vaccinium x Intermedium* Ruthe L.) Leaves. *J Agric Food Chem* 57:9437–9447. <https://doi.org/10.1021/JF9022542>
51. Tsimogiannis D, Samiotaki M, Panayotou G, Oreopoulou V (2007) Characterization of Flavonoid Subgroups and Hydroxy Substitution by HPLC-MS/MS. *Molecules* 2007, Vol. 12, Pages 593–606 12, 593–606. doi:<https://doi.org/10.3390/12030593>
52. Escobar-Avello D, Lozano-Castellón J, Mardones C, Pérez AJ, Saéz V, Riquelme S, Von Baer D, Vallverdú-Queralt A (2019) Phenolic Profile of grape canes: Novel Compounds identified by LC-ESI-LTQ-Orbitrap-MS. *Molecules* 2019 24:3763. <https://doi.org/10.3390/MOLECULES24203763>
53. Yang W, Ye M, Liu M, Kong D, Shi R, Shi X, Zhang K, Wang Q, Lantong Z (2010) A practical strategy for the characterization of Coumarins in *Radix Glehniae* by Liquid Chromatography coupled with Triple Quadrupole-Linear Ion Trap Mass Spectrometry. *J Chromatogr A* 1217:4587–4600. <https://doi.org/10.1016/J.CHROMA.2010.04.076>
54. Serag A, Baky MH, Döll S, Farag MA, UHPLC-MS Metabolome (2019) Based classification of Umbelliferous Fruit Taxa: a Prospect for Phyto-Equivalency of its different accessions and in response to roasting. *RSC Adv* 10:76–85. <https://doi.org/10.1039/C9RA07841J>
55. Martin-Arjol I, Bassas-Galia M, Bermudo E, Garcia F, Manresa A (2010) Identification of oxylipins with antifungal activity by LC-MS/MS from the supernatant of *Pseudomonas* 42A2. *Chem Phys Lipids* 163:341–346. <https://doi.org/10.1016/J.CHEMPHYSLIP.2010.02.003>
56. Alakolanga AGAW, Siriwardene AMDA, Savitri Kumar N, Jayasinghe L, Jaiswal R, Kuhnert N (2014) LC-MSn identification and characterization of the Phenolic Compounds from the fruits of *Flacourtia Indica* (Burm. F.) Merr. And *Flacourtia Inermis* Roxb. *Food Res Int* 62:388–396. <https://doi.org/10.1016/J.FOODRES.2014.03.036>
57. Harnly JM, Bhagwat S, Lin LZ (2007) Profiling methods for the determination of Phenolic Compounds in Foods and Dietary supplements. *Anal Bioanal Chem* 389:47–61. <https://doi.org/10.1007/S00216-007-1424-7/FIGURES/5>
58. Saibabu V, Fatima Z, Khan LA, Hameed S (2015) Therapeutic Potential of Dietary Phenolic Acids. *Adv Pharmacol Sci* 2015, doi:<https://doi.org/10.1155/2015/823539>
59. Panche AN, Diwan AD, Chandra SR, Flavonoids (2016) An overview. *J Nutr Sci* 5:1–15. <https://doi.org/10.1017/JNS.2016.41>
60. Kumadoh D, Kwakye KO, Kuntworbe N, Adi-Dako O, Appenahier JA (2020) Determination of Shelf Life of Four Herbal Medicinal Products using high-performance liquid chromatography analyses of markers and the Systat Sigmaplot Software ARTICLE INFO. *J Appl Pharm Sci* 10:72–080. <https://doi.org/10.7324/JAPS.2020.10610>
61. Müller J, Heindl A (2006) Drying of Medicinal Plants. *Medicinal and Aromatic Plant* 237–252
62. Xu DP, Li Y, Meng X, Zhou T, Zhou Y, Zheng J, Zhang JJ, Li H (2017) Bin Natural Antioxidants in Foods and Medicinal plants: extraction, Assessment and Resources. *Int J Mol Sci* 18. <https://doi.org/10.3390/IJMS18010096>
63. Awah FM, Uzoegwu PN, Oyugi JO, Rutherford J, Ifeonu P, Yao XJ, Fowke KR, Eze MO (2010) Free radical scavenging activity and Immunomodulatory Effect of *Stachytarpheta Angustifolia* Leaf Extract. *Food Chem* 119:1409–1416. <https://doi.org/10.1016/J.FOODCHEM.2009.09.020>
64. Cortés-Rojas DF, Chagas-Paula DA, Da Costa FB, Souza CRF, Oliveira WP (2013) Bioactive Compounds in *Bidens Pilosa* L. populations: a key step in the standardization of Phytopharmaceutical Preparations. *Revista Brasileira de Farmacognosia* 23:28–35. <https://doi.org/10.1590/S0102-695X2012005000100>
65. Wu J, Wan Z, Yi J, Wu Y, Peng W, Wu J (2013) Investigation of the extracts from *Bidens Pilosa* L. and determination of Bioactive Compounds using UHPLC-QqLIT-MS/MS and GC/MS. *BMC Complement Altern Med* 17. <https://doi.org/10.1186/S12906-017-2000-0>
67. Truong DH, Nguyen DH, Ta NTA, Bui AV, Do TH, Nguyen HC (2019) Evaluation of the Use of Different Solvents for Phytochemical Constituents, Antioxidants, and in Vitro Anti-Inflammatory Activities of *Severinia Buxifolia*. *J Food Qual* 2019, doi:<https://doi.org/10.1155/2019/8178294>
68. Musicki B, Periers AM, Laurin P, Ferroud D, Benedetti Y, Lachaud S, Chateaux F, Haesslein JL, Iltis A, Pierre C et al (2000) Improved antibacterial activities of Coumarin Antibiotics Bearing 5',5'-Dialkylnoviose: Biological Activity of RU79115. *Bioorg Med Chem Lett* 10:1695–1699. [https://doi.org/10.1016/S0960-894X\(00\)00304-8](https://doi.org/10.1016/S0960-894X(00)00304-8)
69. Tosun A, Akkol EK, Yeşilada E (2009) Anti-inflammatory and antinociceptive activity of Coumarins from *Seseli Gummiferum* Subsp. *Corymbosum* (Apiaceae). *Z fur Naturforschung - Sect C J Biosci* 64:56–62. <https://doi.org/10.1515/ZNC-2009-1-210/MACHINEREADABLECITATION/RIS>
70. Bartnik M, Facey PC, Glycosides (2017) *Pharmacognosy: Fundamentals, Applications and Strategy* 101–161, doi:<https://doi.org/10.1016/B978-0-12-802104-0.00008-1>
71. Akkol EK, Genç Y, Karpuz B, Sobarzo-Sánchez E, Capasso R (2020) Coumarins and coumarin-related Compounds in Pharmacotherapy of Cancer. *Cancers (Basel)* 12:1–25. <https://doi.org/10.3390/CANCERS12071959>
72. Escher B, Neale P, Leusch F (2021) Bioanalytical Tools in Water Quality Assessment. *Bioanalytical Tools in Water Quality Assessment*. <https://doi.org/10.2166/9781789061987>
73. Sak K (2014) Cytotoxicity of Dietary Flavonoids on different human Cancer types. *Pharmacogn Rev* 8. <https://doi.org/10.4103/0973-7847.134247>
74. Xu M, Fujita D, Kajiwara S, Minowa T, Li X, Takemura T, Iwai H (2010) Hanagata, N. Contribution of Physicochemical characteristics of Nano-Oxides to cytotoxicity. *Biomaterials* 31:8022–8031. <https://doi.org/10.1016/J.BIOMATERIALS.2010.06.022>
75. Abdel-Ghany RH, Barakat WM, Shahat AA, Abd-Allah WES, Ali EA (2016) In Vitro and in vivo hepatoprotective activity of extracts of Aerial Parts of *Bidens Pilosa* L. (Asteraceae). *Trop J Pharm Res* 15:2371–2381. <https://doi.org/10.4314/tjpr.v15i11.11>

Publisher's Note Springer Nature remains neutral with regard to jurisdictional claims in published maps and institutional affiliations.

Springer Nature or its licensor (e.g. a society or other partner) holds exclusive rights to this article under a publishing agreement with the author(s) or other rightsholder(s); author self-archiving of the accepted manuscript version of this article is solely governed by the terms of such publishing agreement and applicable law.